

Supplementary data

New benzimidazole, 1,2,4-triazole and 1,3,5-triazine – based derivatives as potential EGFR^{WT} and EGFR^{T790M} inhibitors: microwave assisted synthesis, anticancer evaluation and molecular docking study

Heba E. Hashem ¹, Abd El-Galil E. Amr ^{2,3}, Eman S. Nossier ⁴, Manal M. Anwar ^{5*},
Eman M. Azmy ¹

¹Department of Chemistry, Faculty of Women, Ain Shams University, Heliopolis, Cairo 11757, Egypt.

²Pharmaceutical Chemistry Department, Drug Exploration & Development Chair (DEDC), College of Pharmacy, King Saud University, Riyadh 11451, Saudi Arabia.

³Applied Organic Chemistry Department, National Research Center, Cairo, Dokki 12622, Egypt.

⁴ Pharmaceutical Medicinal Chemistry and Drug Design Department, Faculty of Pharmacy (Girls), Al-Azhar University, Cairo 11754, Egypt.

⁵Department of Therapeutic Chemistry, National Research Centre, Dokki, Cairo 12622, Egypt.

*** Corresponding author:**

E-mail addresses: manal.hasan52@live.com

Contents:

Experimental; chemistry, *In-vitro* cytotoxic assay (MTT), *In vitro* inhibition assay of EGFR^{WT}, and mutant EGFR^{T790M} activities, *In vivo* determination of p53 ubiquitination, Molecular modeling study on EGFR^{WT}, and mutant EGFR^{T790M}, ¹H-NMR spectra of the new compounds, ¹³C-NMR spectra of the new compounds, IR spectra of the new compounds, Mass spectra of the new compounds.

4.Experimental**4.1.Chemistry**

All melting points were determined on a Gallenkamp apparatus and are uncorrected. Microwave irradiation reactions were performed using a Galanz microwave oven, WP1000AP30-2 (1000 watt, 30-80% of its total power) at Chemistry Department, Faculty of Women, Ain Shams University. The IR spectra were measured on a Pye-UnicamSP300 instrument in potassium bromide discs. The ¹H-NMR and ¹³C-

NMR spectra were recorded on Varian Mercury VX (400 MHz) spectrometer (with operating frequencies 500 MHz for ^1H using TMS as an internal standard and 125 MHz for ^{13}C). Chemical shifts (δ) are reported in parts per million (ppm) and coupling constants (J) are reported in Hertz (Hz). NMR spectra were referenced to the residual signals of DMSO- d_6 . Mass spectra were run on a MAT Finnigan SSQ 7000 spectrometer, using the electron impact technique (EI). Elemental analyses were carried out by the Micro analytical Center of Cairo University, Giza, Egypt. The progression of the reactions was monitored using TLC Merck Kieselgel 60 F254 aluminum packed plates.

4.2. Biological activity

4.2.1. *In vitro* cytotoxic assay (MTT)

The potential cytotoxic properties of the prepared compounds **2-8** were evaluated against a battery of different cell lines, including hepatocellular carcinoma (HepG2), prostate carcinoma (PC3), breast adenocarcinoma (MCF-7), non-small cell lung cancer cells (A549) and the normal peripheral blood mononuclear cells (PBMC). Compounds **2-8** were tested using standard MTT assay⁹⁸, depending on the development of purple formazan crystals by mitochondrial dehydrogenases. Cells were propagated under standard cultivation conditions in RPMI 1640 medium supported with 5% FBS and 2 mM L-glutamine. Upon testing, only cell batched with viabilities over 95% were used. Briefly, cells were inoculated into 96-well plates to a final concentration of 2×10^4 cells/well/100 μl , and the plates were incubated for 24 h at 37°C, 5% CO_2 , 95% relative humidity. Afterwards, exhausted media were aspirated and serial dilutions of the different compounds prepared in DMSO were added to each well, and incubation was allowed for another 48 h. DMSO was used as the negative control, and different positive controls (Doxorubicin, DOX; Cytarabine, CYT; Bicalutamide, BIC; Paclitaxel, PAC; Epirubicin, EPI; Gemcitabine, GEM) were used depending on cell line type. Accordingly, 20 μl MTT (5 mg/ml, PBS) were added to each well, and plates were incubated for another 4 h, then the contents of each well were carefully aspirated and DMSO was added (100 μl /well). Plates were shaken to dissolve the formed crystals and then the absorbance was read at 570 nm. IC_{50} values defining the concentration inhibiting 50% of viable cell growth were obtained from linear regression of the dose-response curves using Origin 6.1 software (Origin Lab Corporation, Northampton, MA, USA). All experiments were performed thrice for result reproducibility.

4.2.2. *In vitro* inhibition assay of EGFR^{WT}, and mutant EGFR^{T790M} activities

All the compounds were further examined for their inhibitory activities against both EGFR^{WT} and EGFR^{T790M}. Homogeneous time resolved fluorescence (HTRF) assay^{99,100} was applied in this test with EGFR^{WT} and EGFR^{T790M} (Sigma). Firstly, EGFR^{WT} and/or EGFR^{T790M} and their substrates were incubated with the tested compounds in enzymatic buffer for 5 min. ATP (1.65 μM) was added into the reaction mixture to allow starting the enzymatic reaction. The assay was conducted for 30 min at room temperature. The reaction was stopped by the addition of detection reagents which contain EDTA. The detection step continued for 1 h, and then the IC₅₀ values were determined using GraphPad Prism 5.0. Three independent experiments were performed for each concentration.

4.2.3. *In vivo* determination of p53 ubiquitination

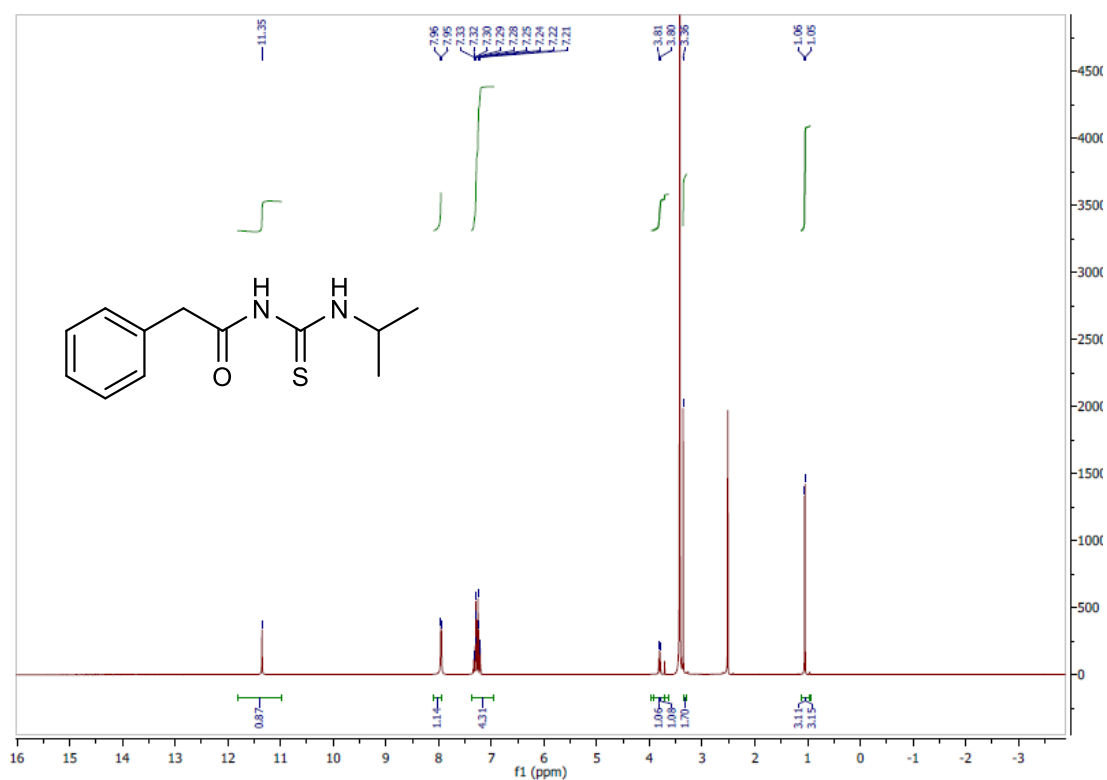
The potential of different prepared derivatives as potent p53 ubiquitination inhibitors was evaluated using standard procedure and protocol previously applied^{101,102}. Briefly, cells were allowed to grow for 24 h to reach 50% confluency. Thereafter, of 1 μg p53, 4 μg MDM2 and 1 μg HIS-ubiquitin were transfected with Gene Juice reagent, and then cells were grown for another 20 h. Afterwards, cells were treated with different derivatives or controls for 6 h and MG132 for 4 h, then washed and collected in PBS, where 5% of the solution was kept as an input. The remaining pelleted cells (95% after centrifugation) were lysed in 700 μL of ubiquitin buffer A (6 M guanidinium HCl, 300 mM NaCl, 50 mM phosphate pH 8.0, 100 μg/mL N-ethylmaleimide), and sonicated for 5 min at 20% amplitude. Lysates were incubated overnight with Invitrogen Dynabeads His-Tag matrix and washed once with ubiquitin buffers A, B, C and phosphate buffered saline (ubiquitin buffer B: Mix ubiquitin buffer A and ubiquitin buffer C 1:1; ubiquitin buffer C: 300 mM NaCl, 50 mM phosphate pH 8.0, 100 μg/mL N-ethylmaleimide). The washed lysates were resolved by 8% sodium dodecyl sulfate–polyacrylamide gel electrophoresis, followed by immunoblotting with a p53 (DO-1) antibody. Diphenyl imidazole was used as a positive control.

4.3. Molecular modeling study on EGFR^{WT}, and mutant EGFR^{T790M}

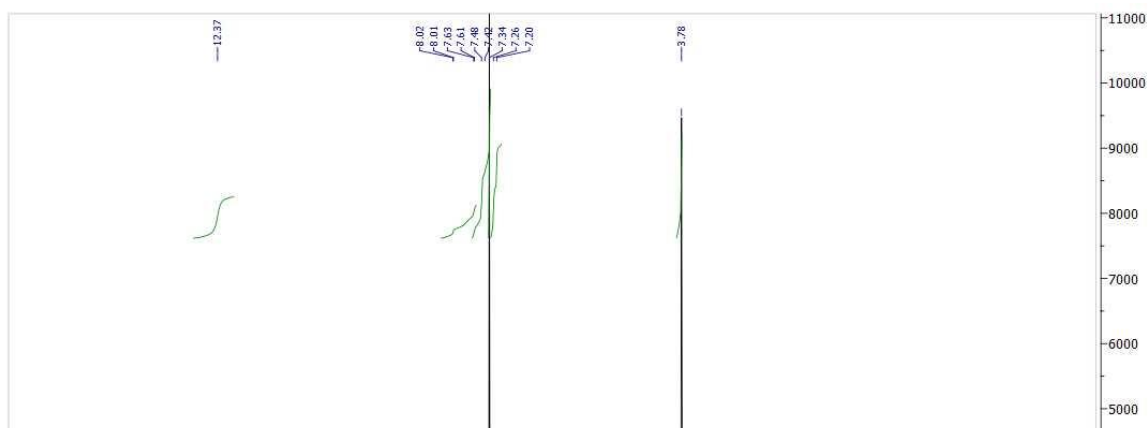
In the current docking simulation, compound **6b** was chosen based on the potency and scaffold type in order to correlate the structure-activity relationship with its behavior and the possible binding interactions within the active site of EGFR^{WT}, and mutant EGFR^{T790M}. Thus, the domains of EGFR^{WT}, and mutant EGFR^{T790M} kinase complexed with erlotinib and AZD9291 (PDB ID: IM17 and 6JX0)^{103,104} was downloaded from the protein data bank. The docking calculations were done using

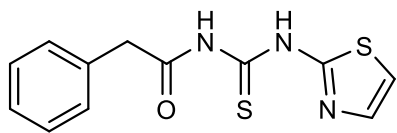
MOE-Dock (Molecular Operating Environment) software version 2014.0901^{105,106}. At the beginning, redocking of the native ligands (erlotinib and AZD9291) was achieved within their own binding sites of EGFRWT and EGFR790M giving energy scores - 11.40 and -12.66 kcal/mol with RMDS values (root mean square deviation) 0.91 and 1.02 Å, respectively.

¹H-NMR spectra of the new compounds:

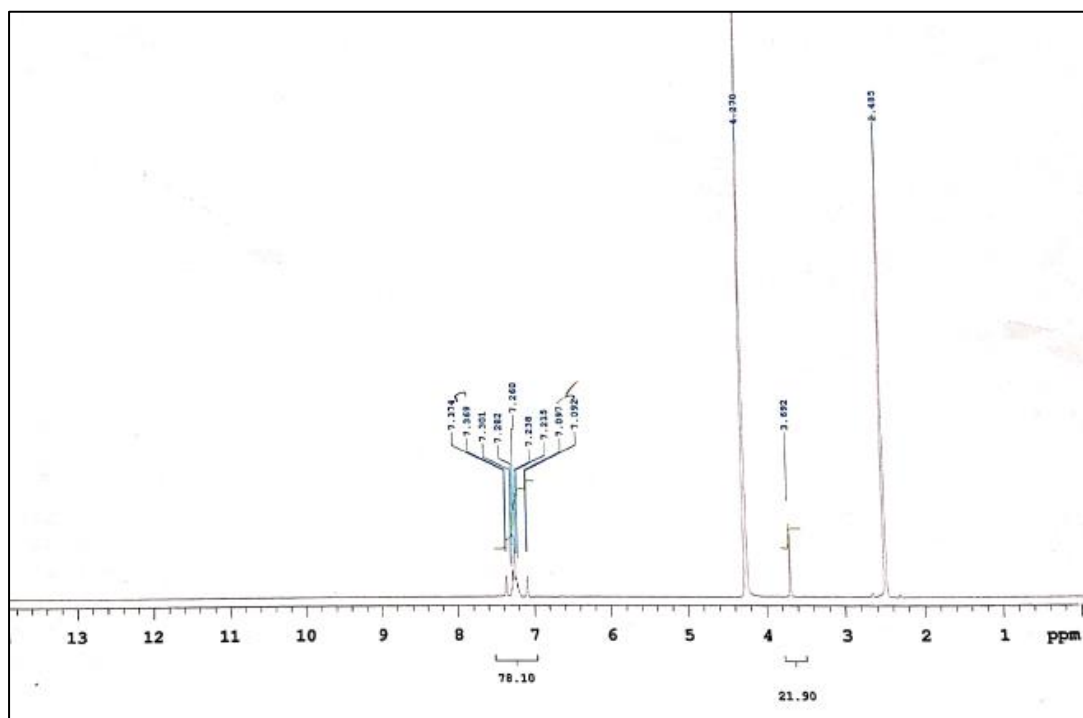


S1: Compound 2a

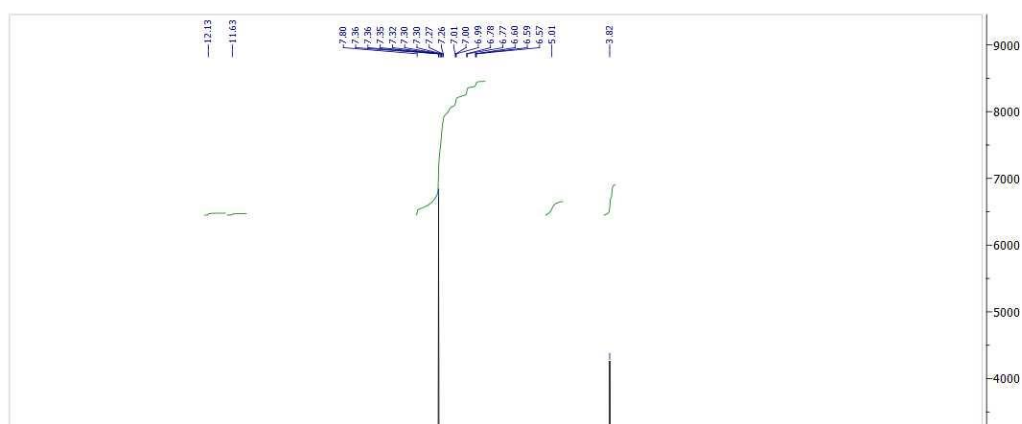


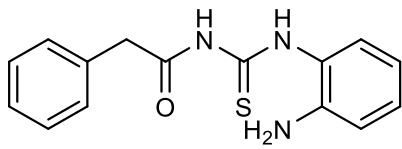


S2: Compound 2b

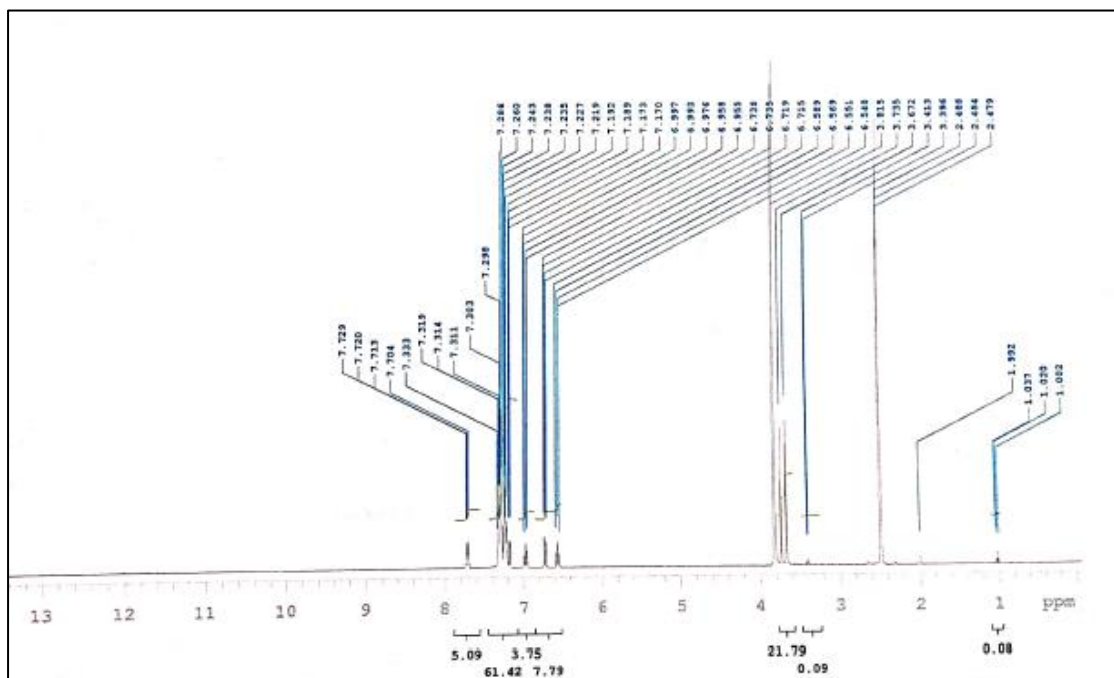


S3: Compound 2b- D₂O

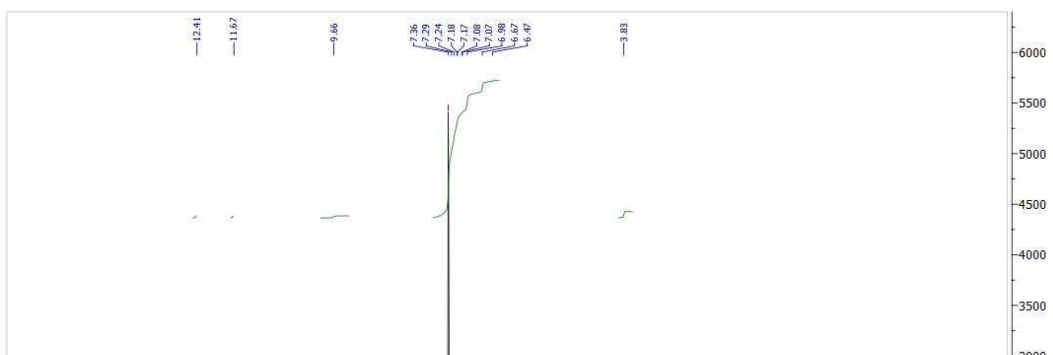


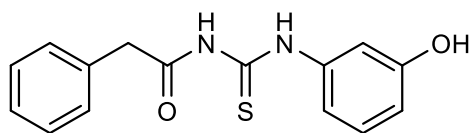


S4: Compound 2c

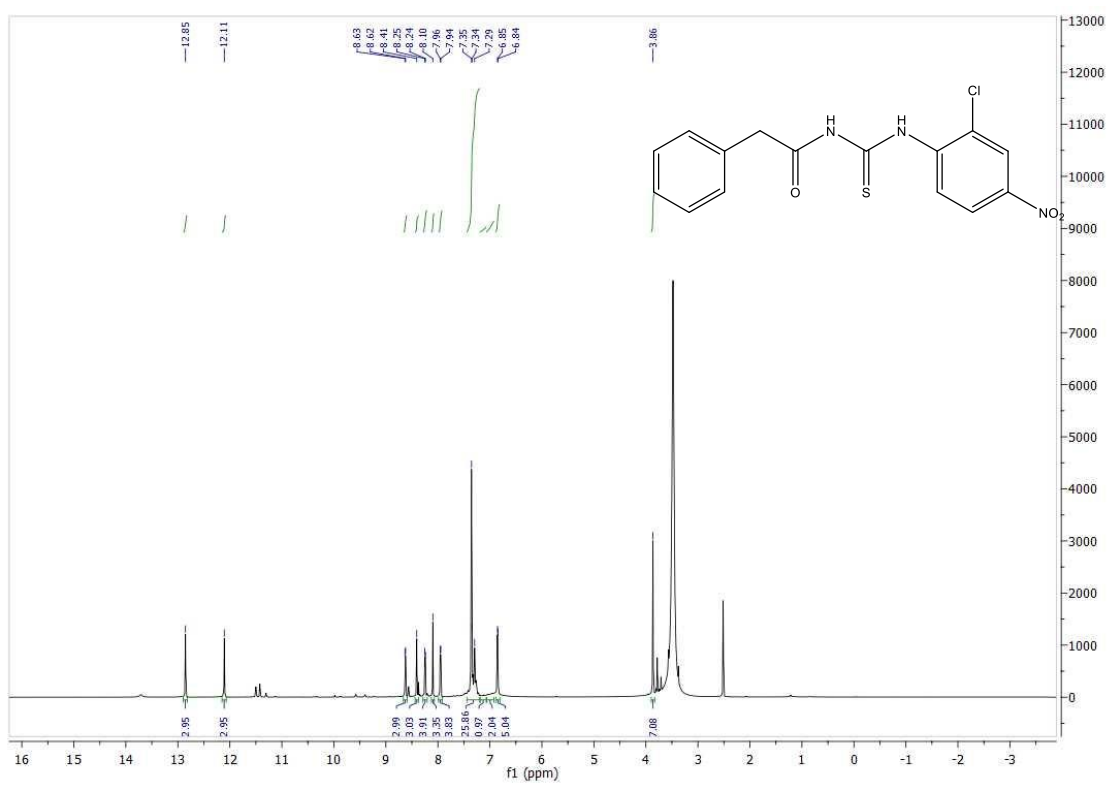


S5: Compound 2c- D₂O

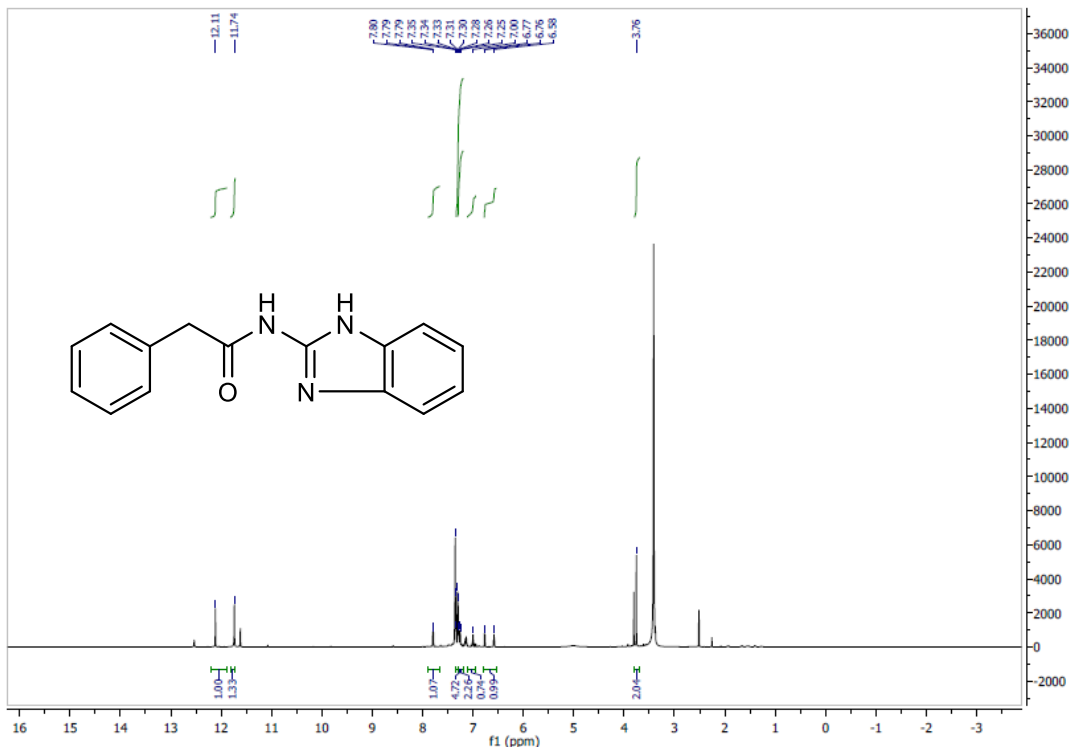




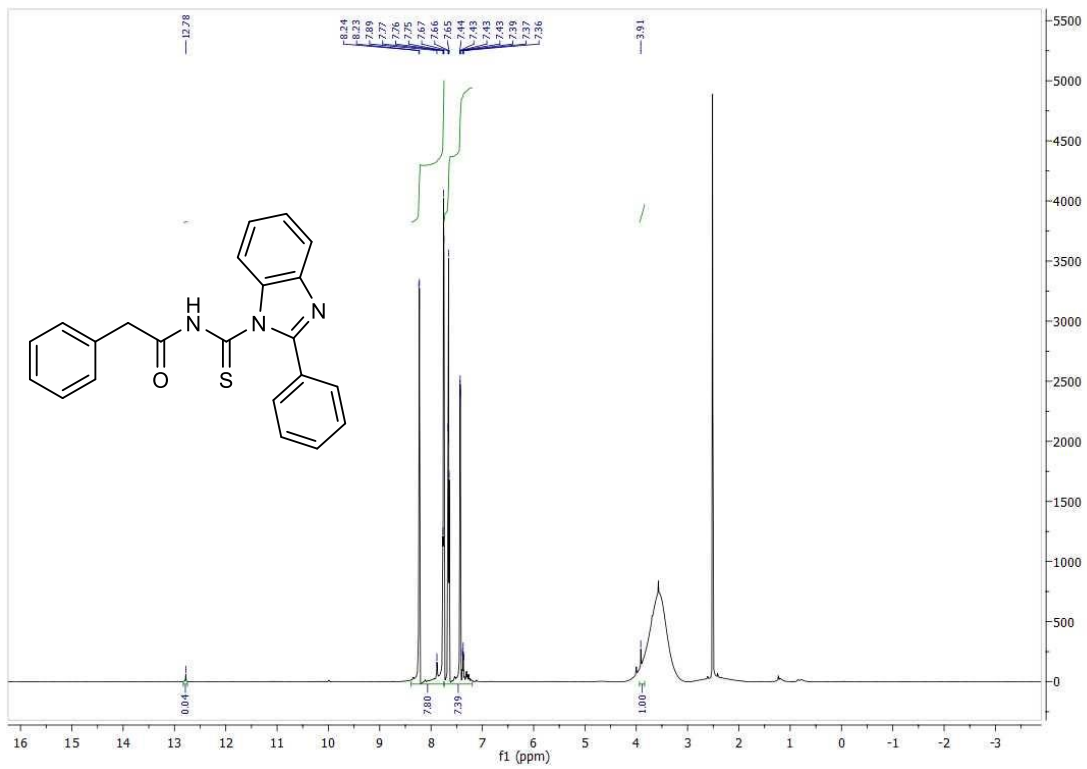
S6: Compound 2d



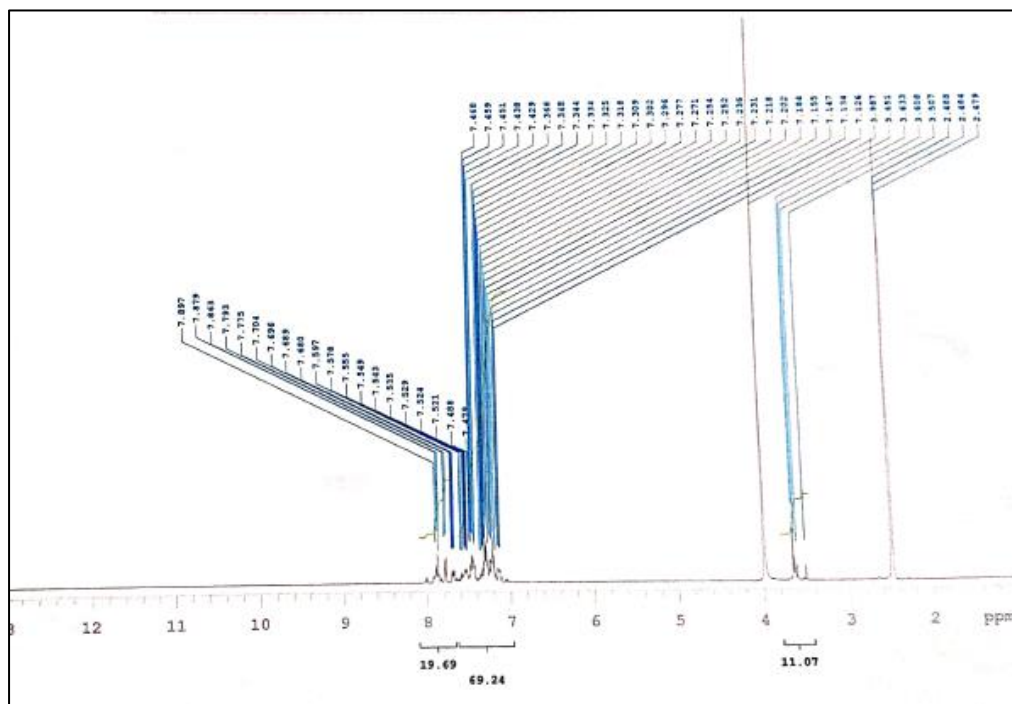
S7: Compound 2e



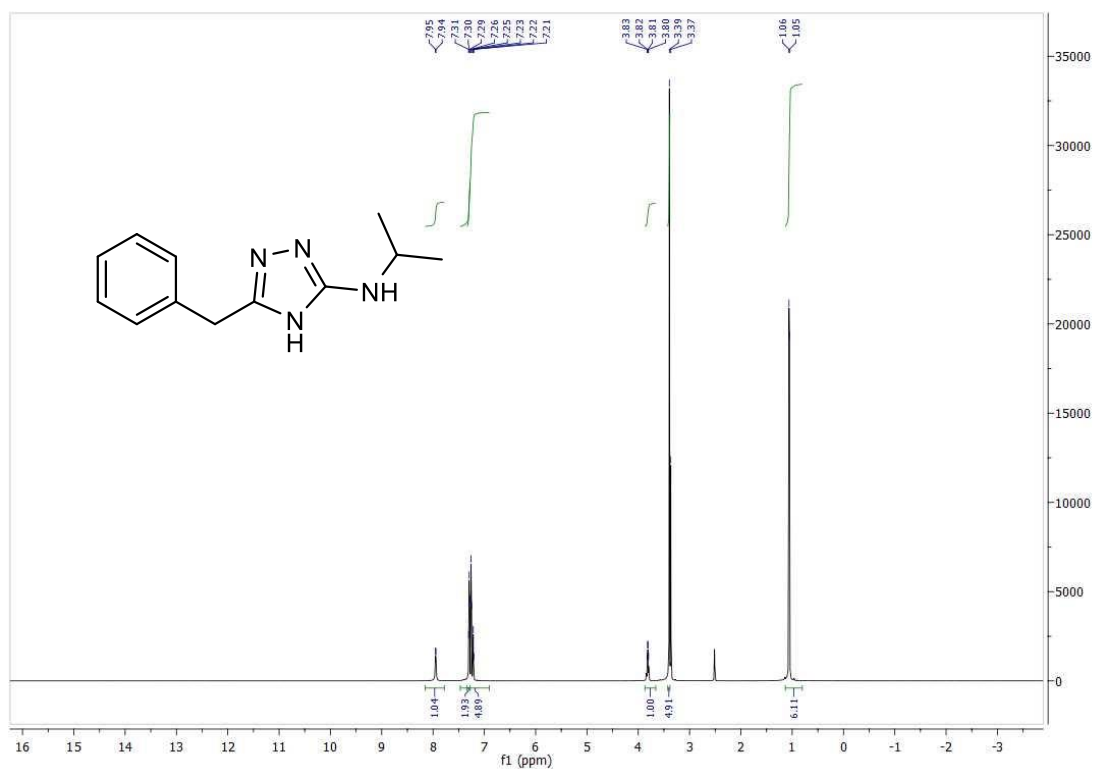
S8: Compound 3



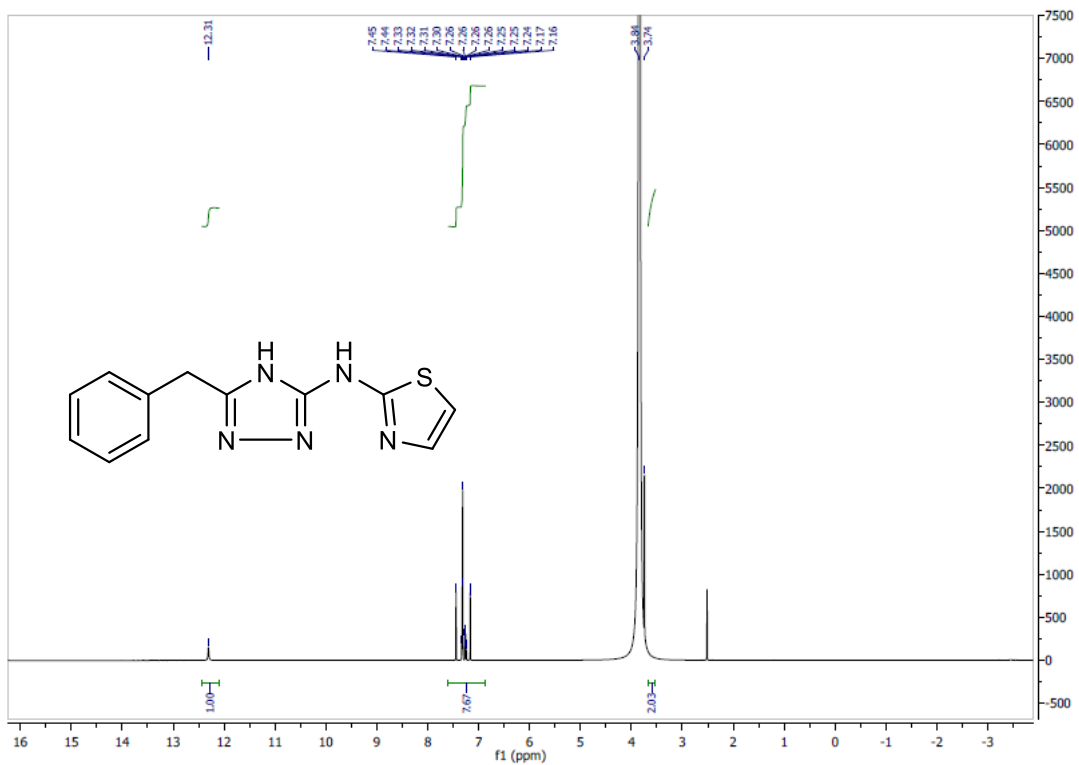
S9: Compound 4



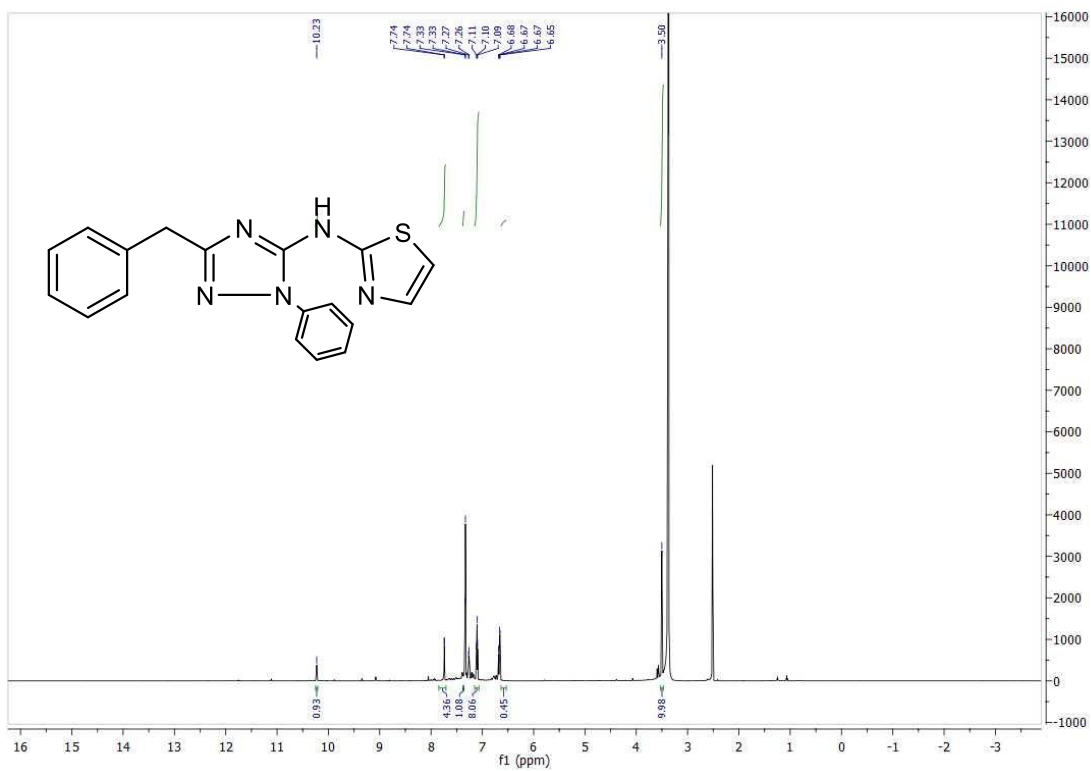
S10: Compound 4- D₂O



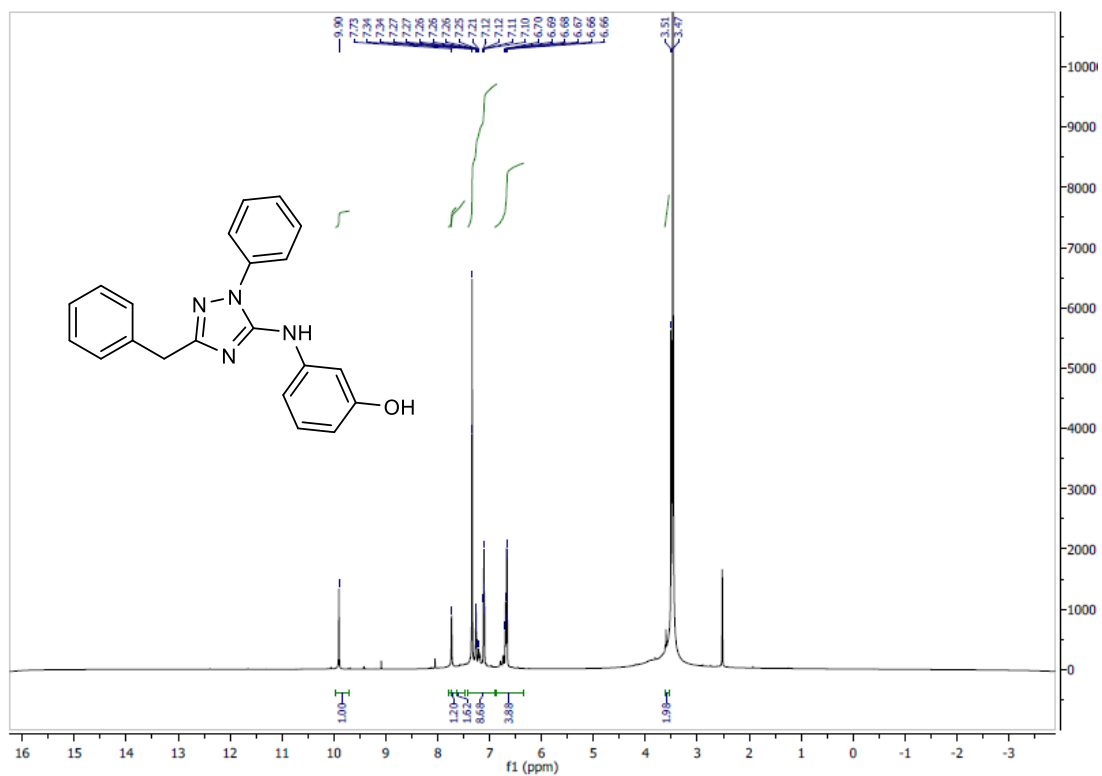
S11: Compound 5a



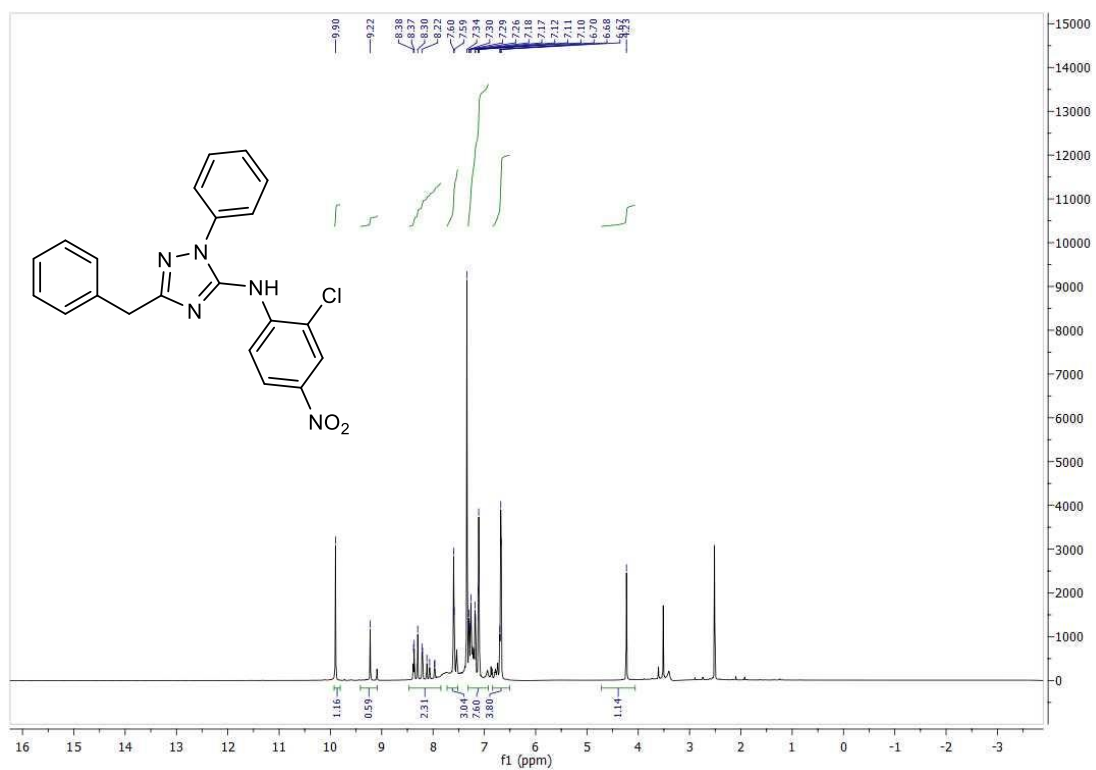
S12: Compound 5b



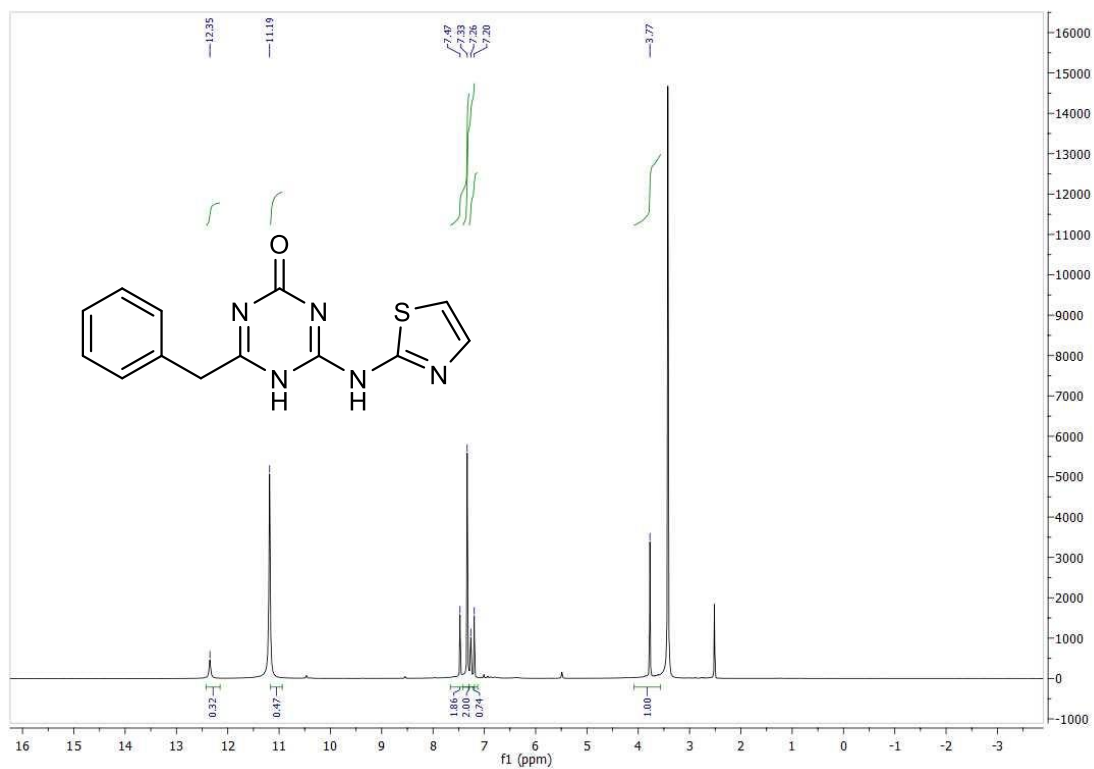
S13: Compound 6a



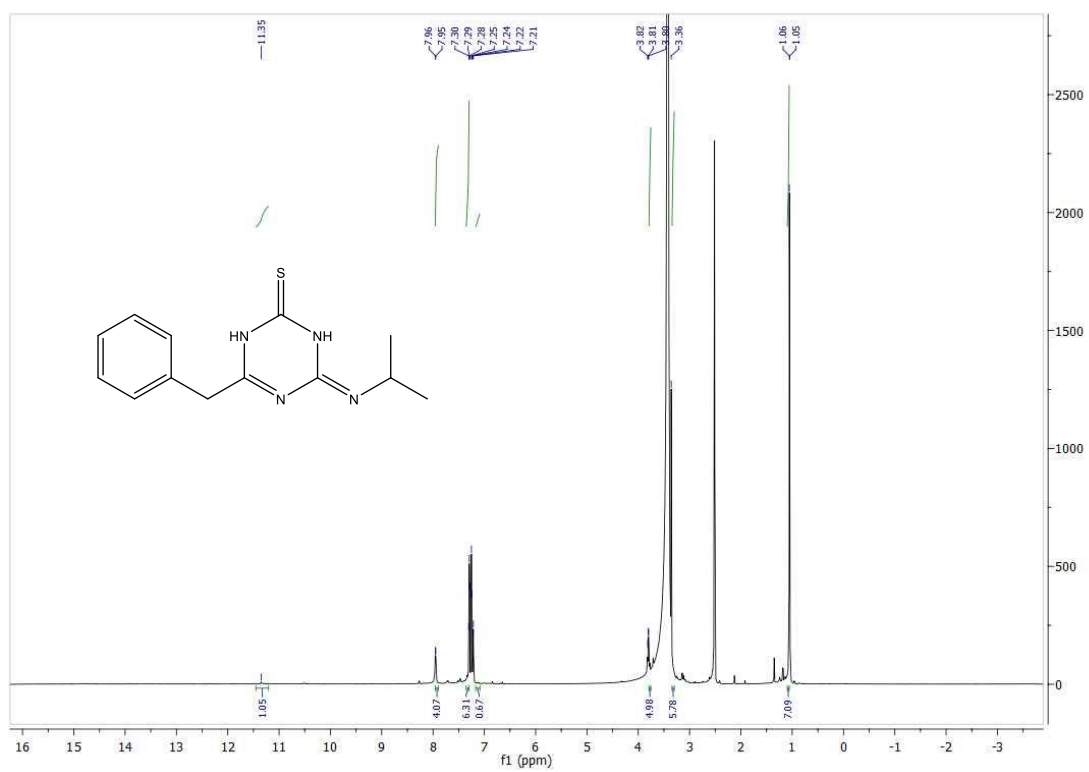
S14: Compound 6b



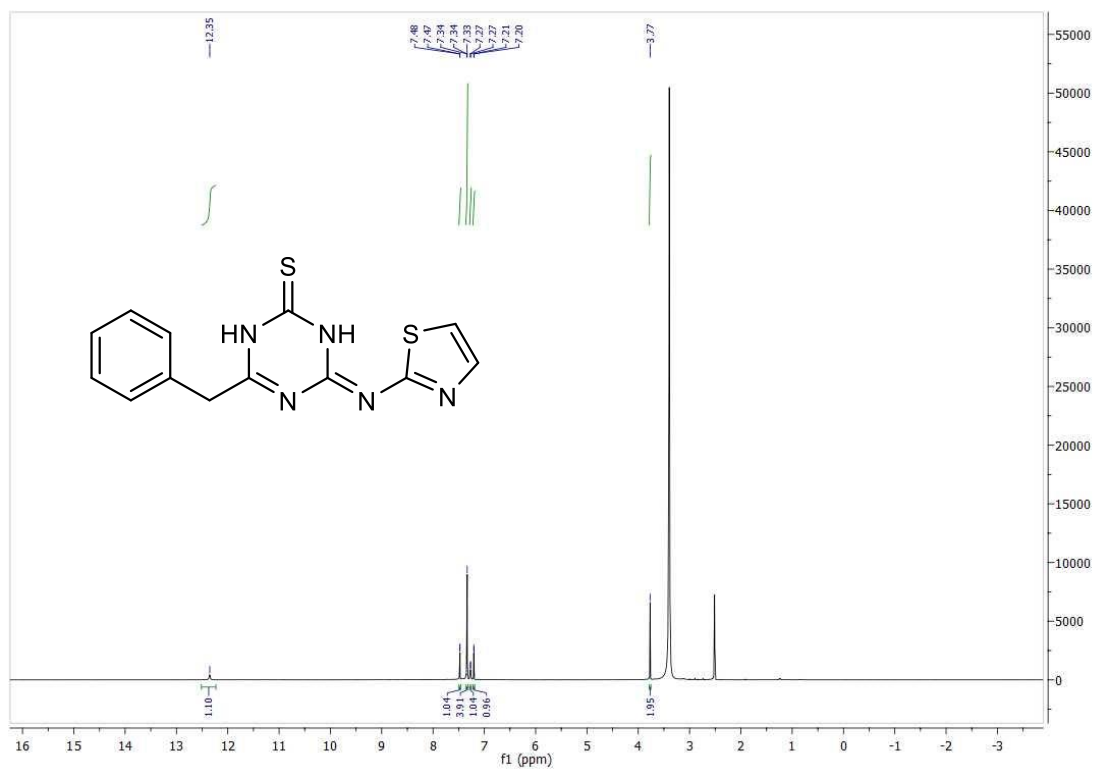
S15: Compound 6c



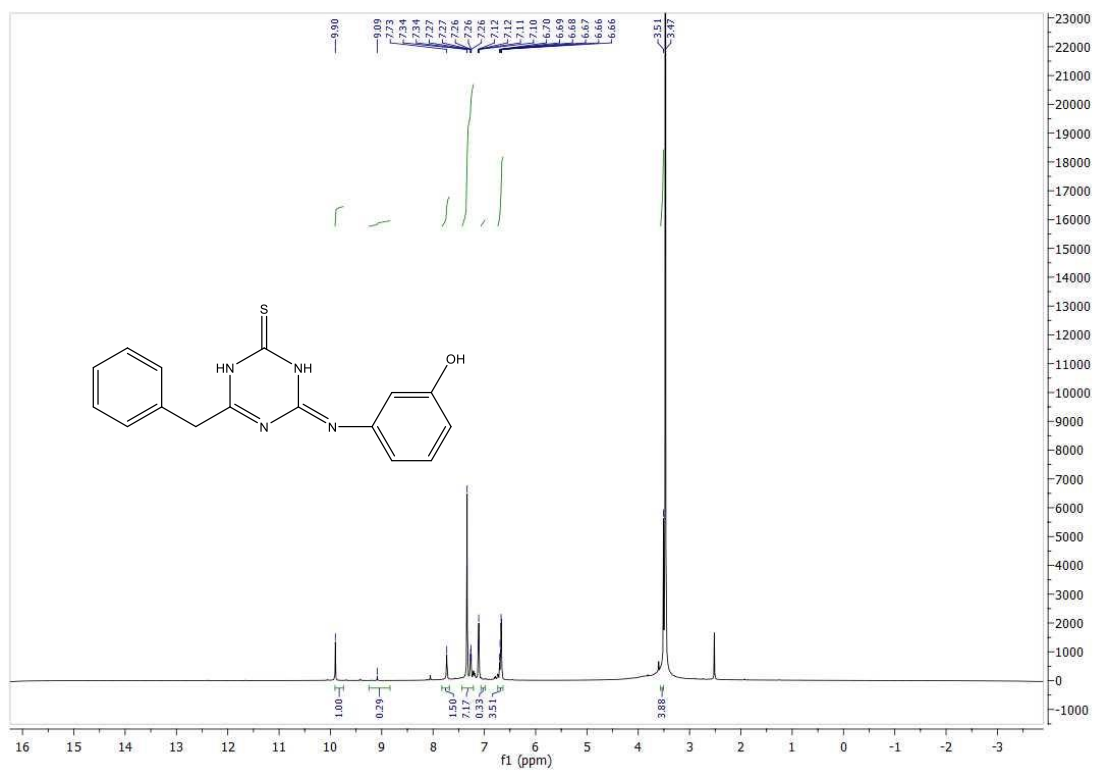
S16: Compound 7



S17: Compound 8a

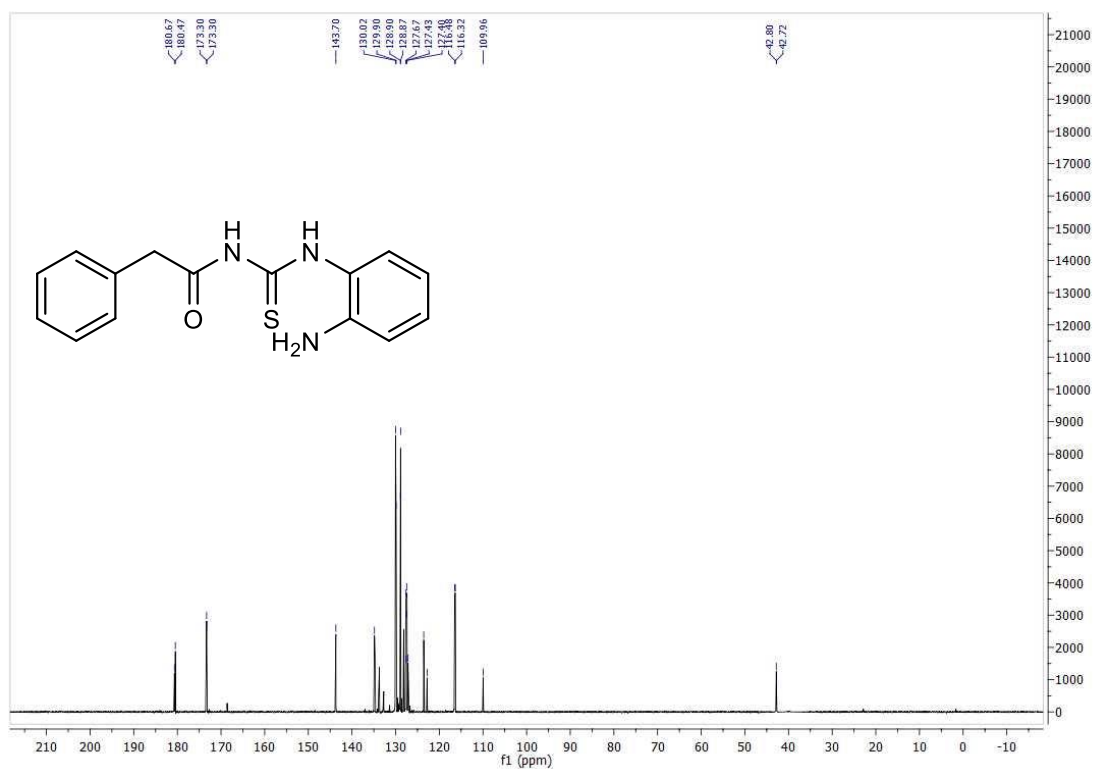


S18: Compound 8b

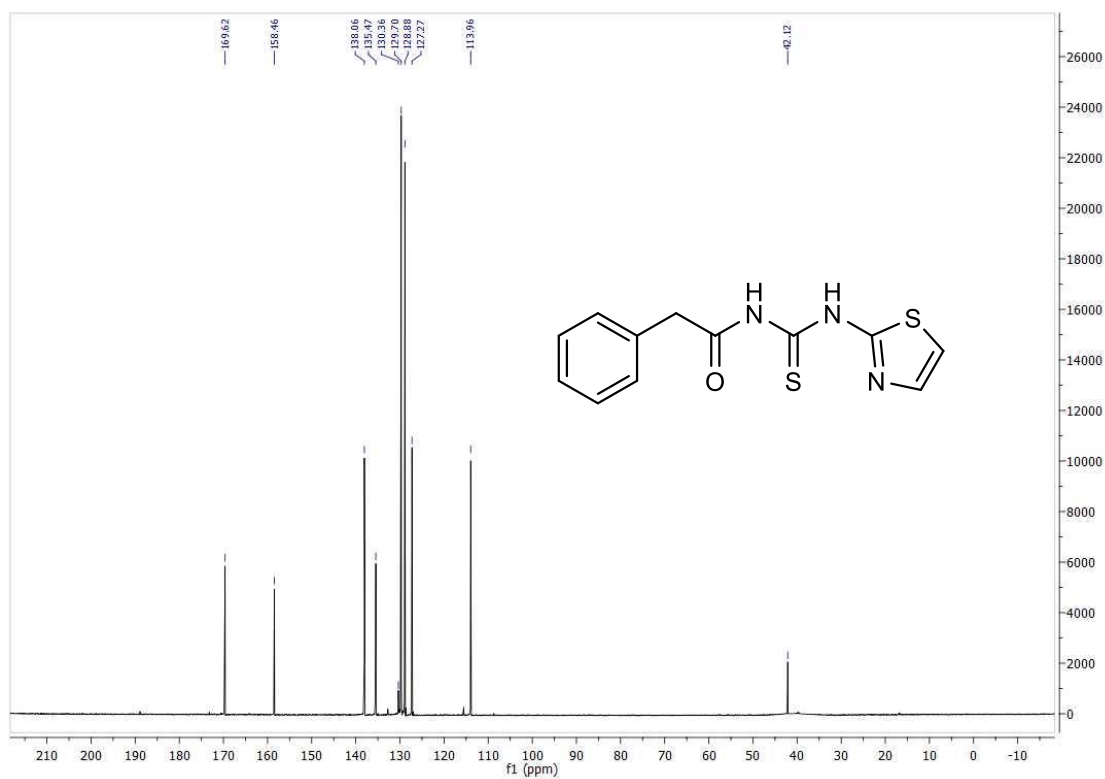


S19: Compound 8c

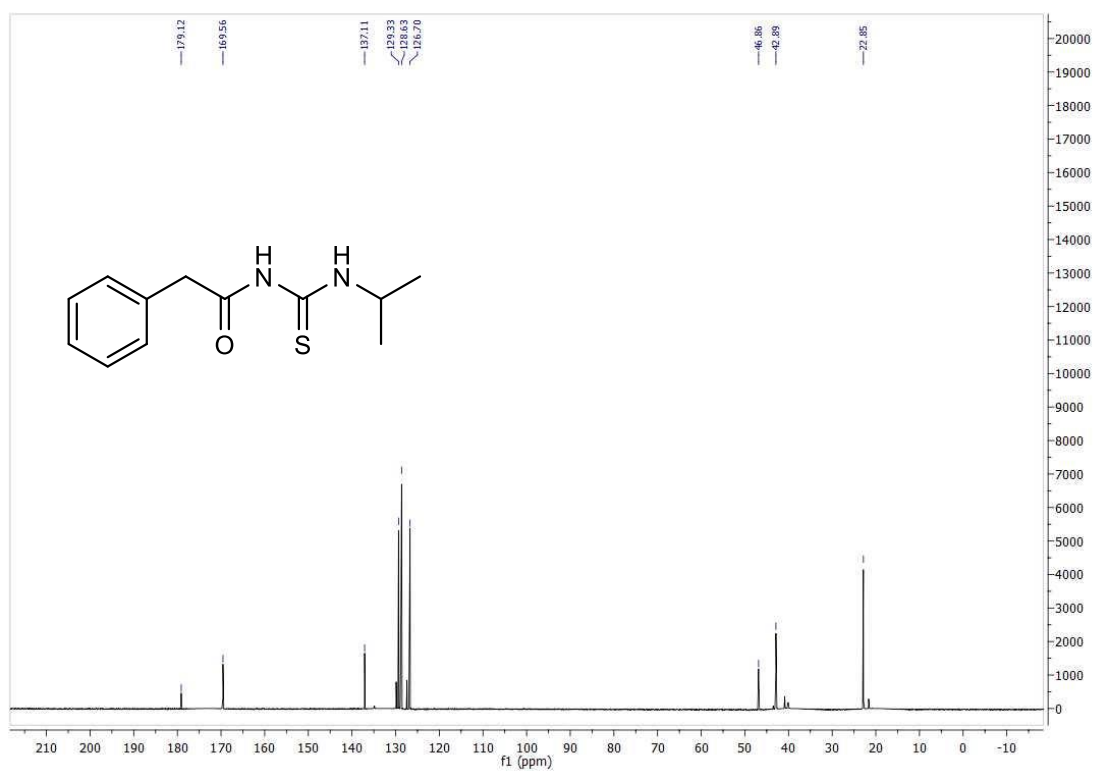
¹³C-NMR spectra of the new compounds:



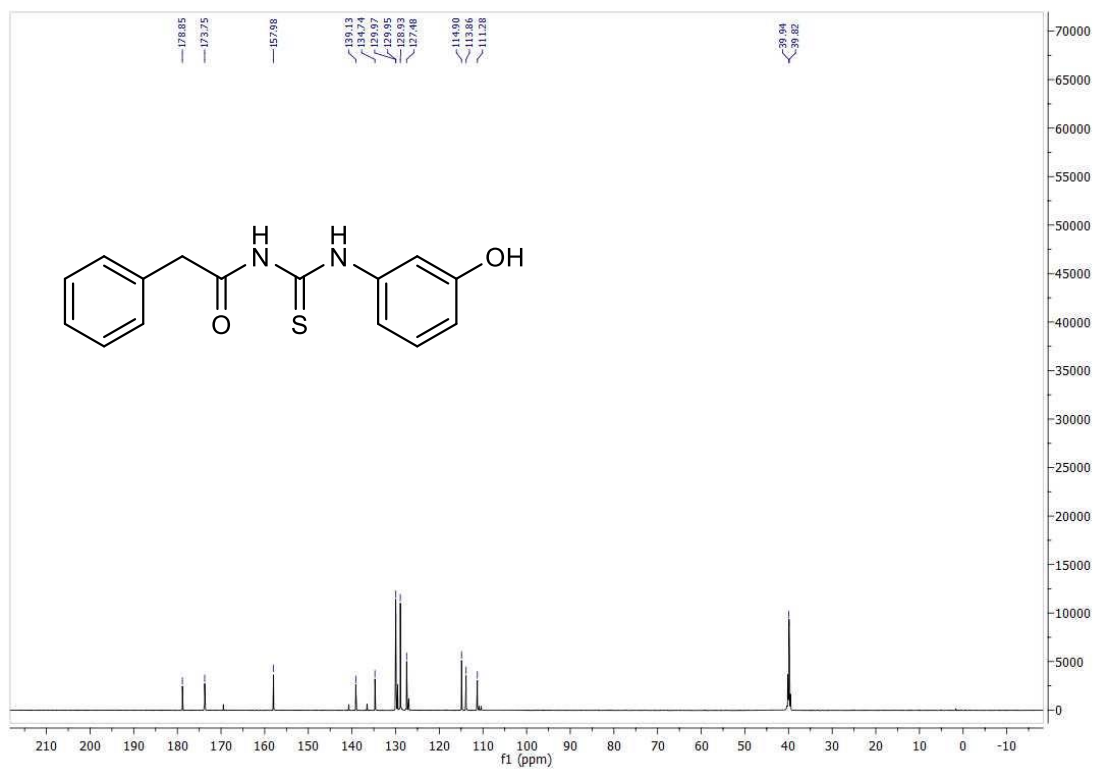
S20: Compound 2c



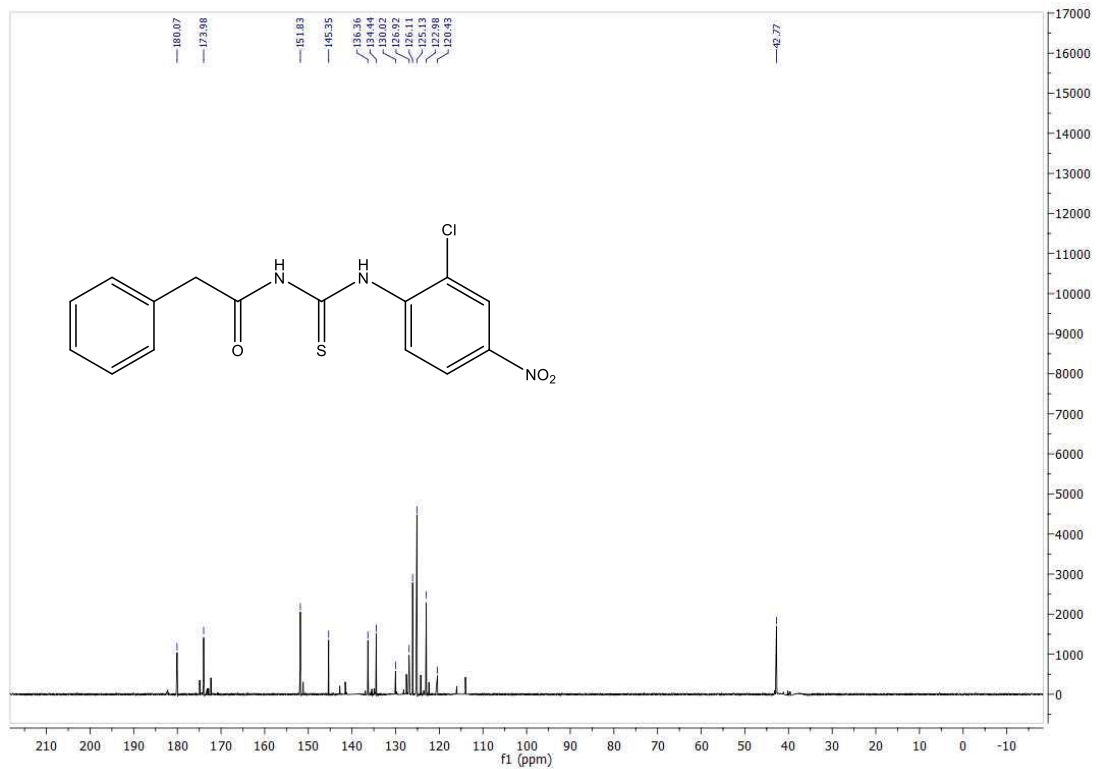
S21: Compound 2b



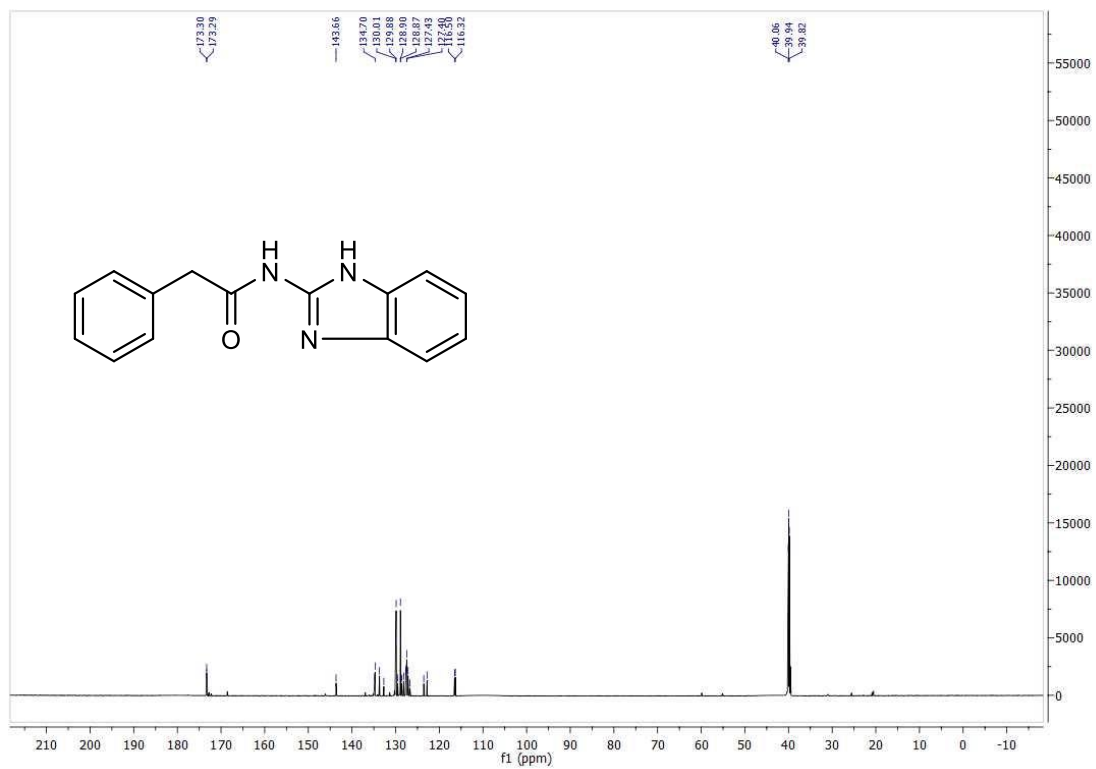
S22: Compound 2a



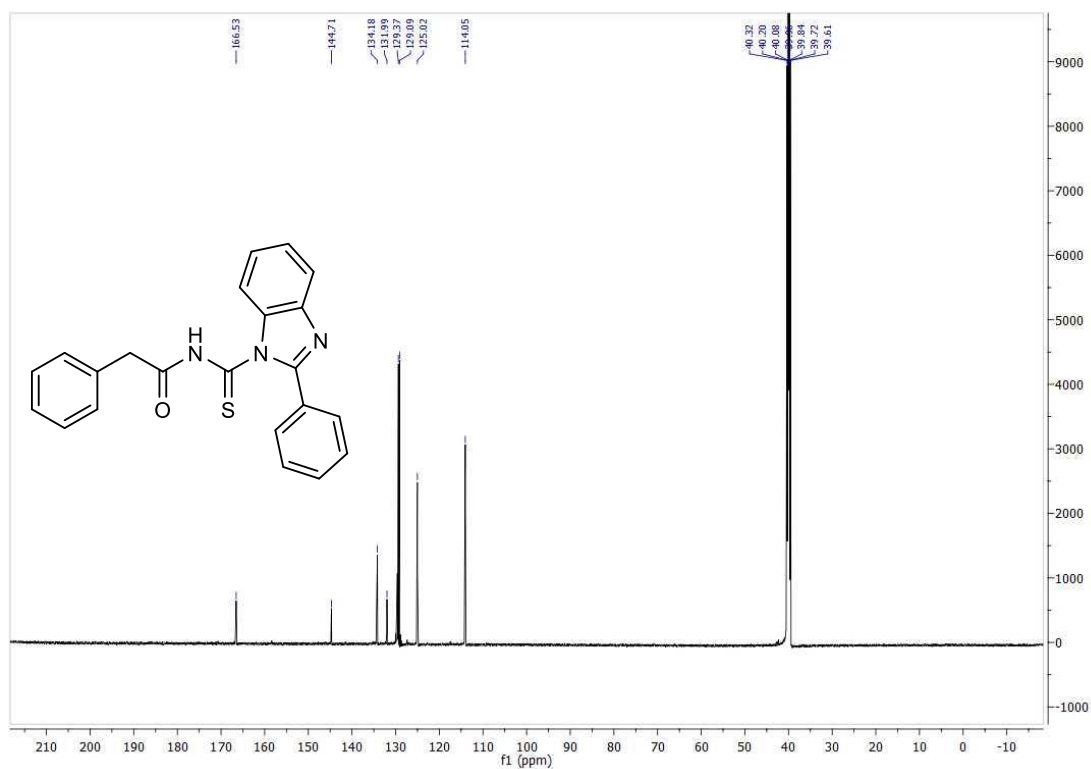
S23: Compound 2d



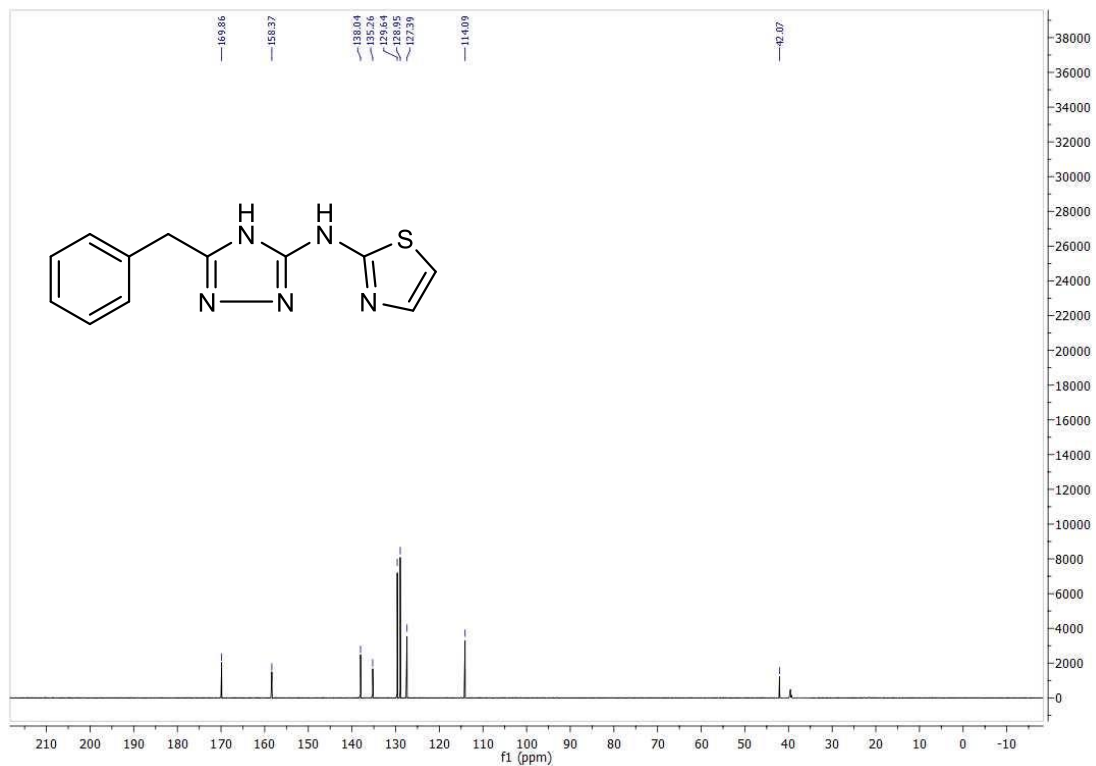
S24: Compound 2e



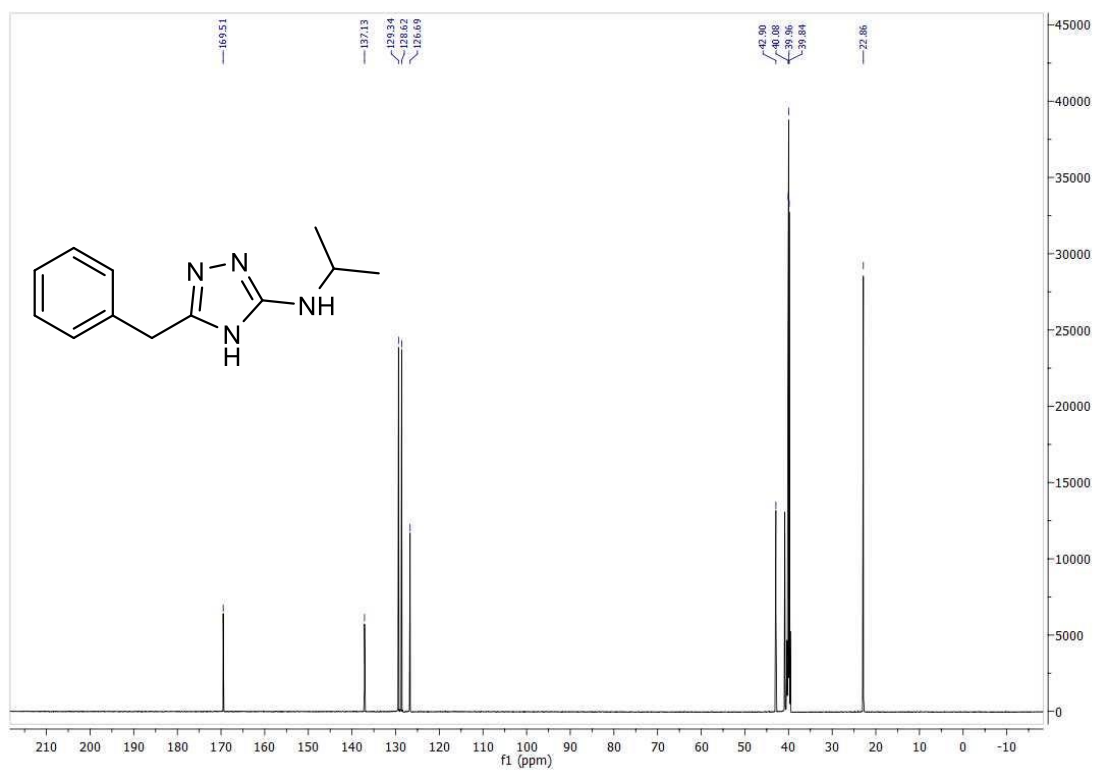
S25: Compound 3



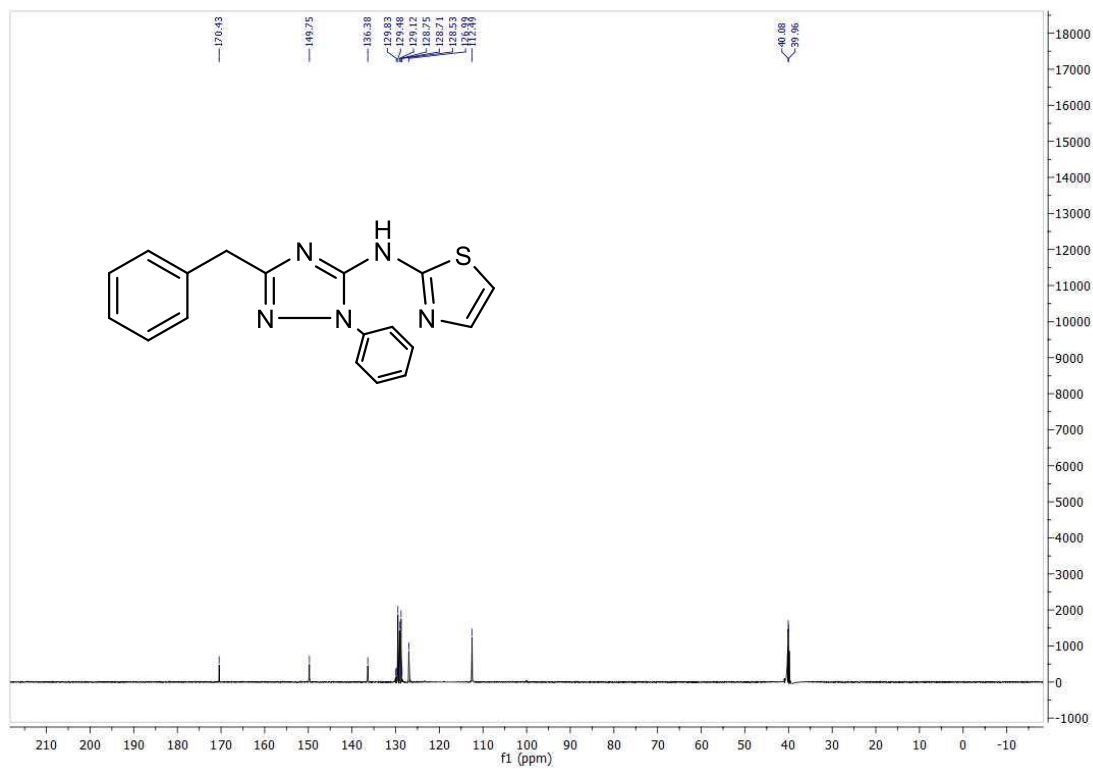
S26: Compound 4



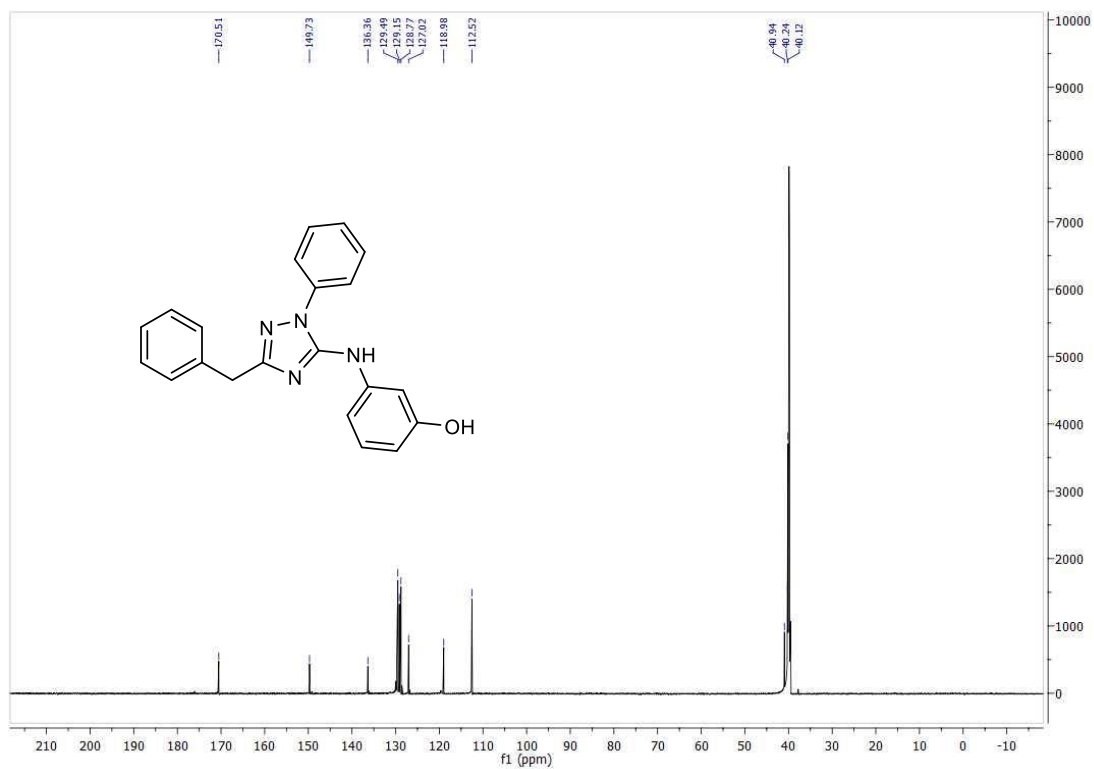
S27: Compound 5b



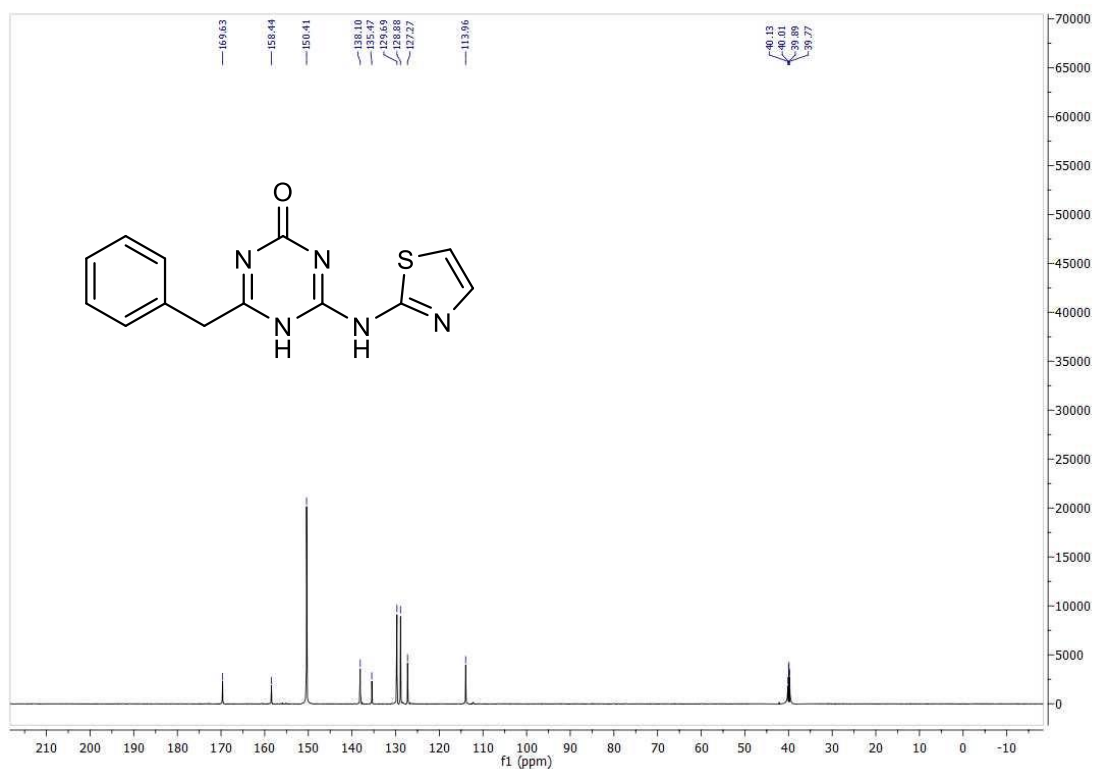
S28: Compound 5a



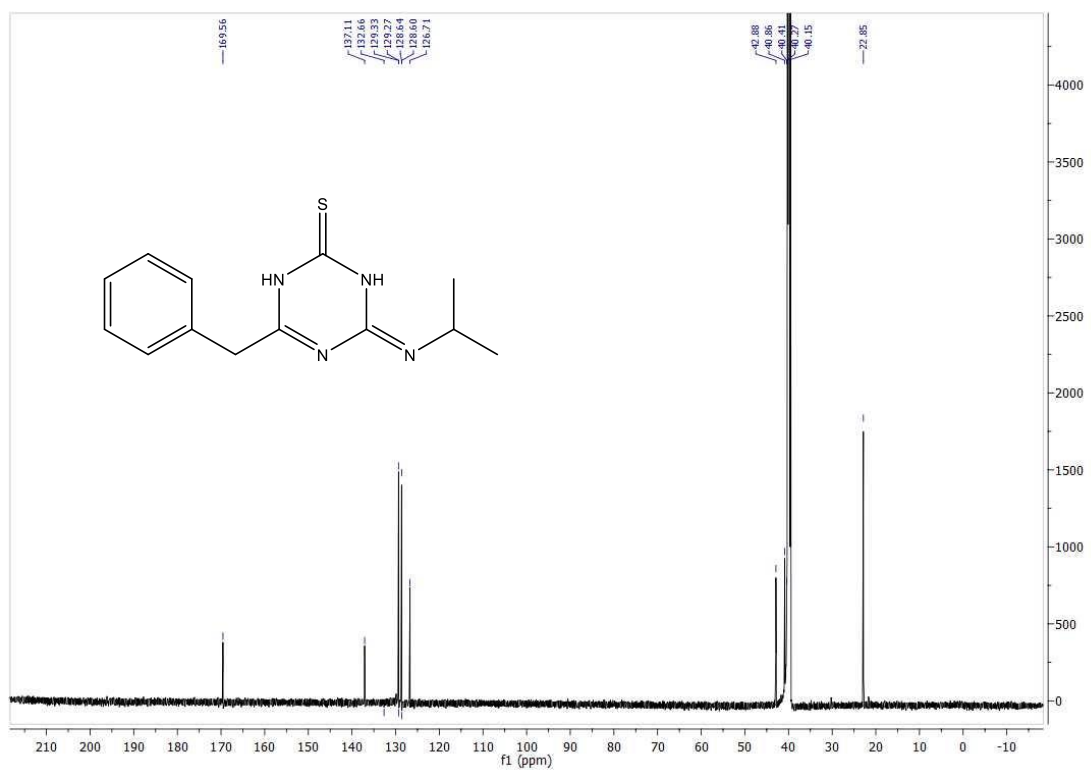
S29: Compound 6a



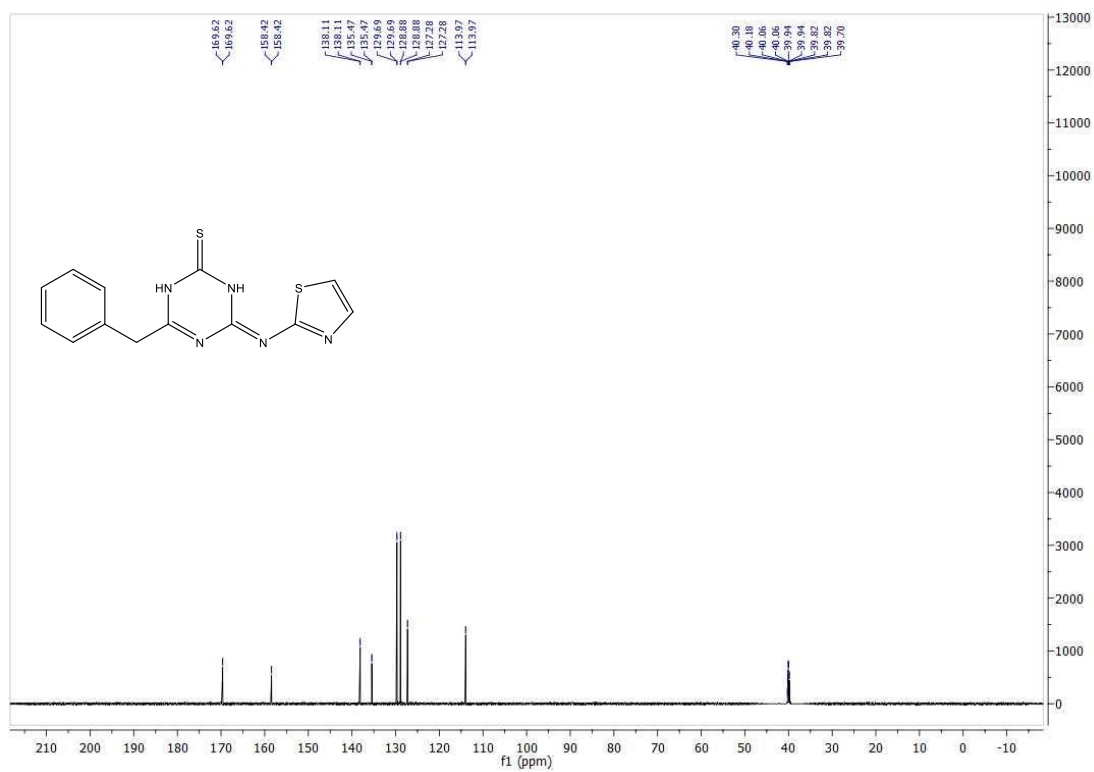
S30: Compound 6b



S31: Compound 7

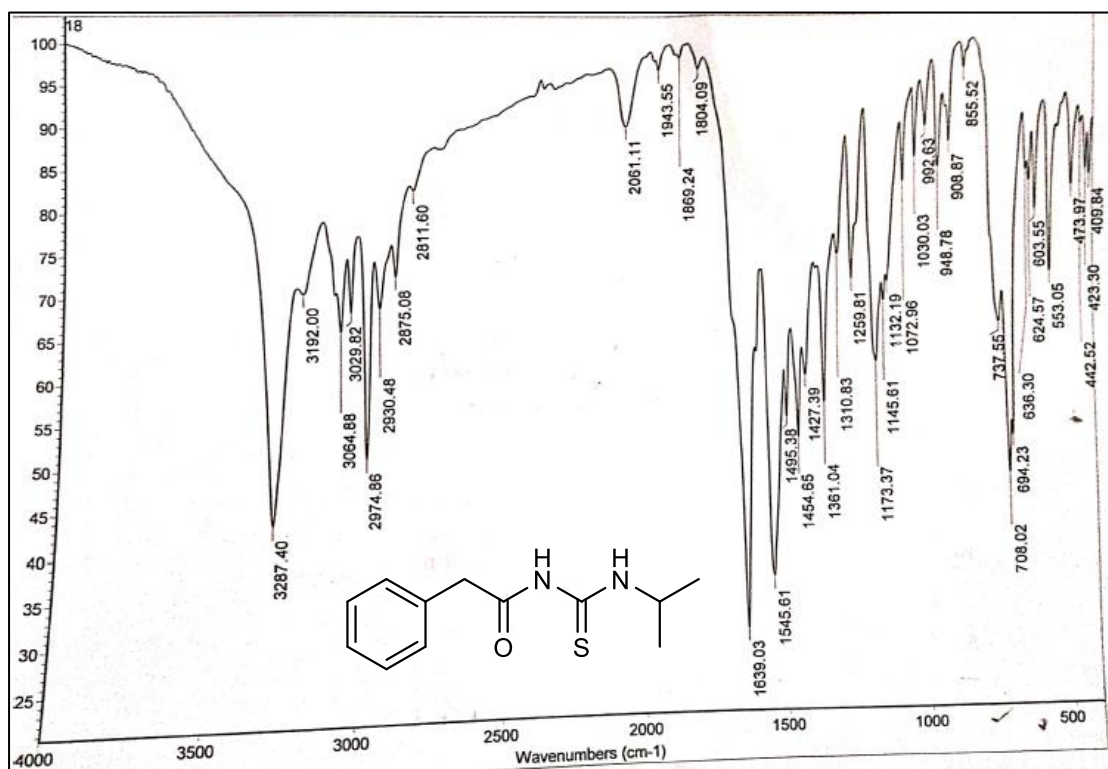


S32: Compound 8a

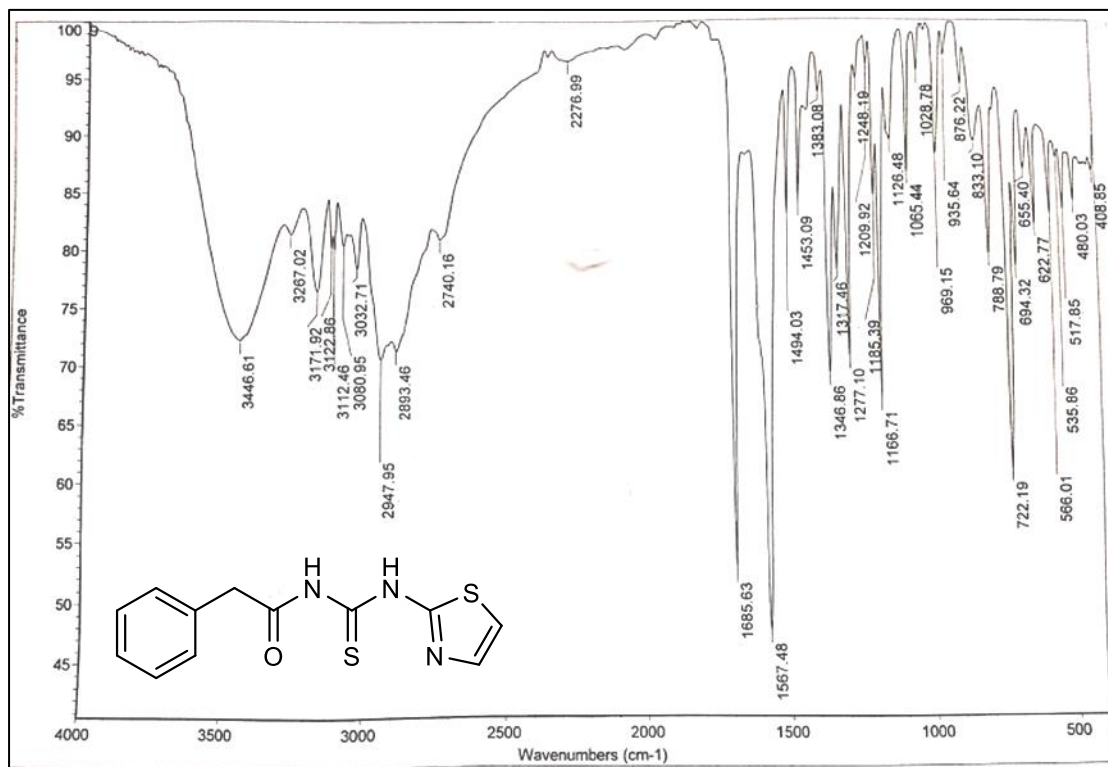


S33: Compound 8b

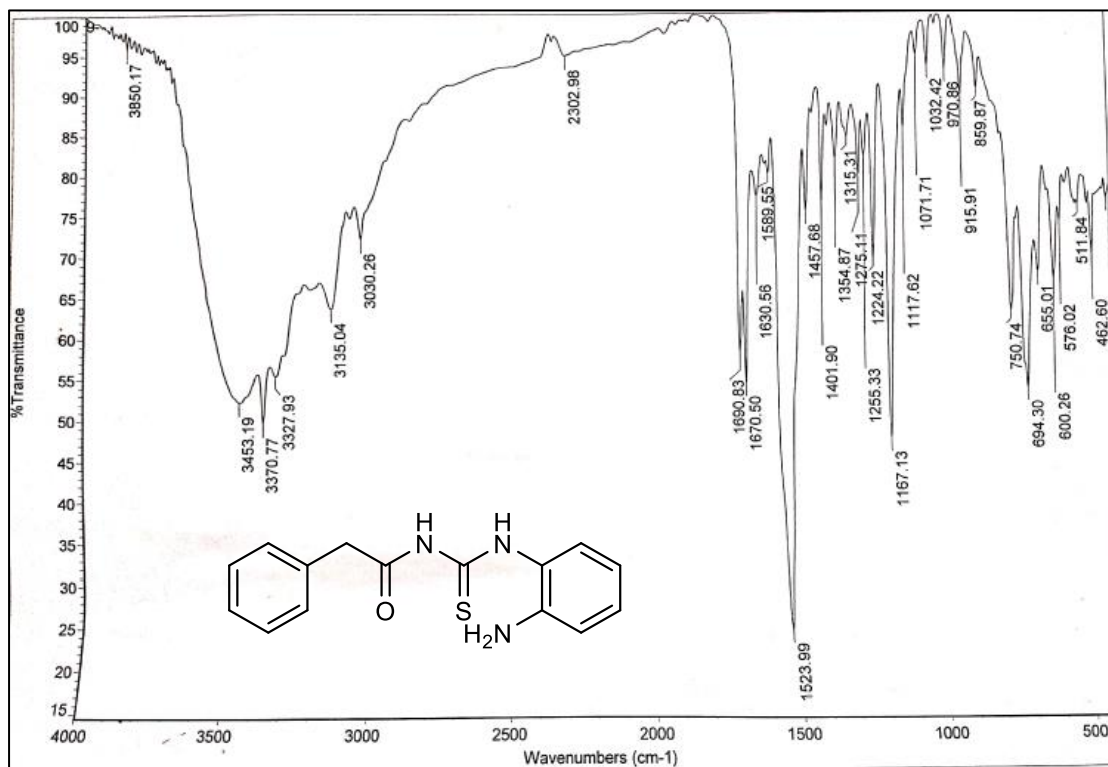
IR spectra of the new compounds:



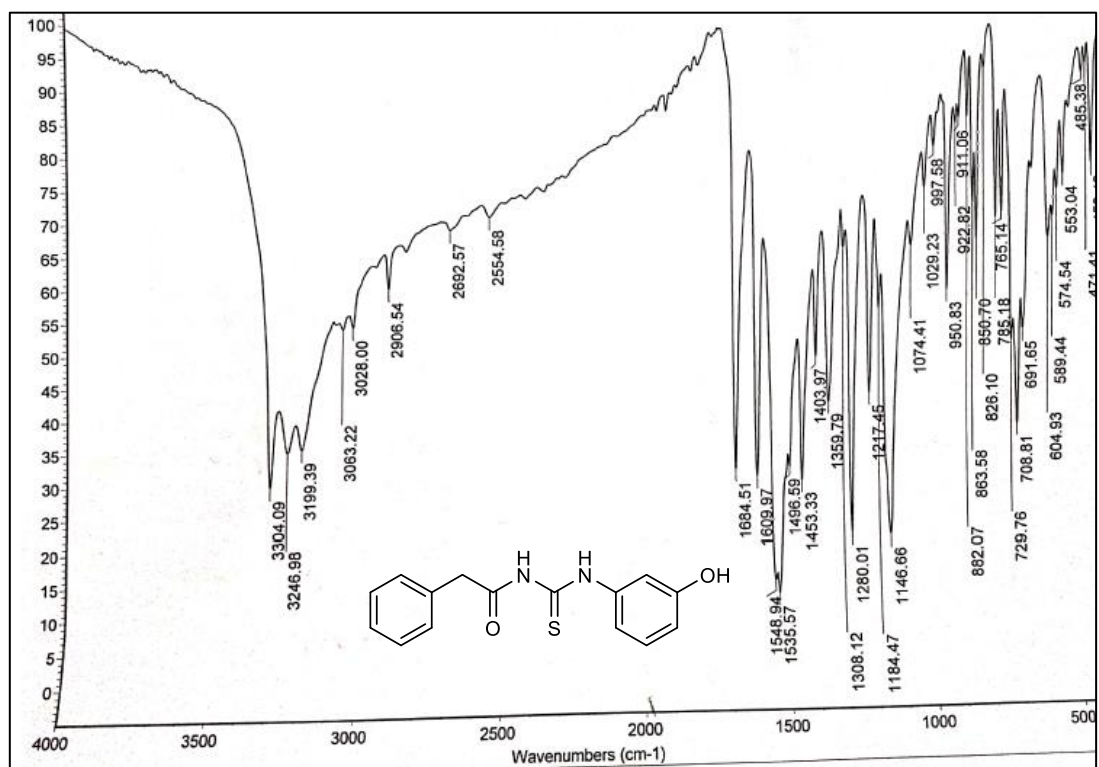
S34: Compound 2a



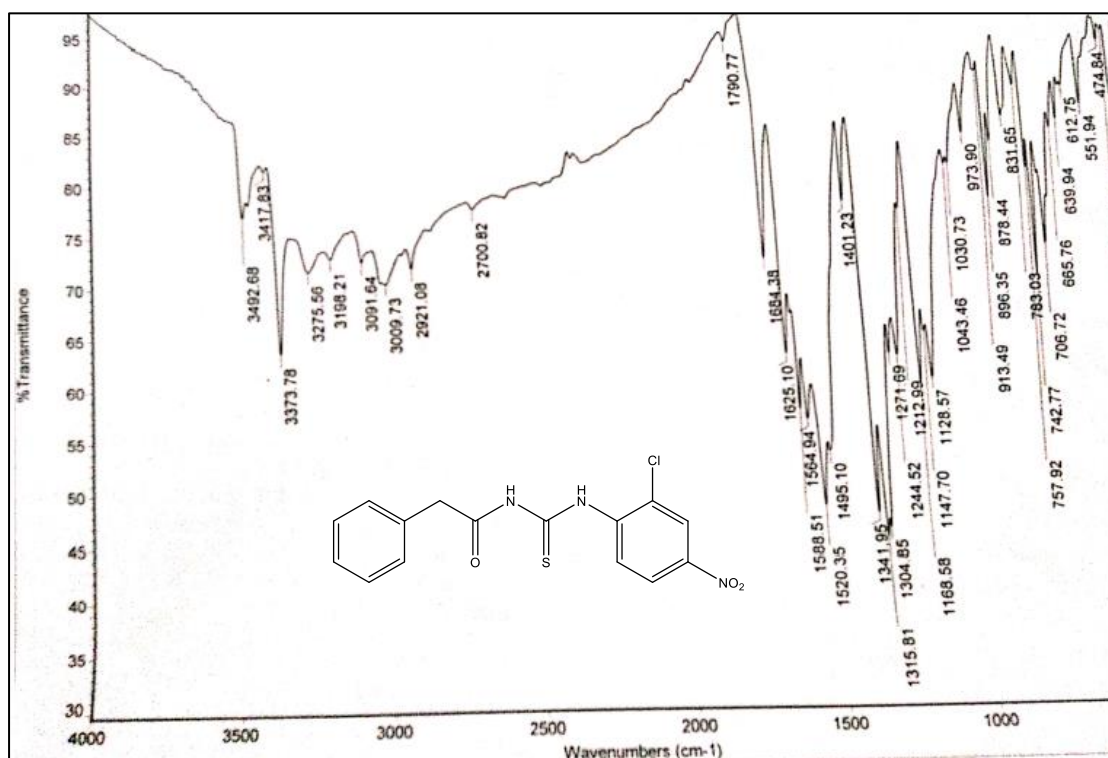
S35: Compound 2b



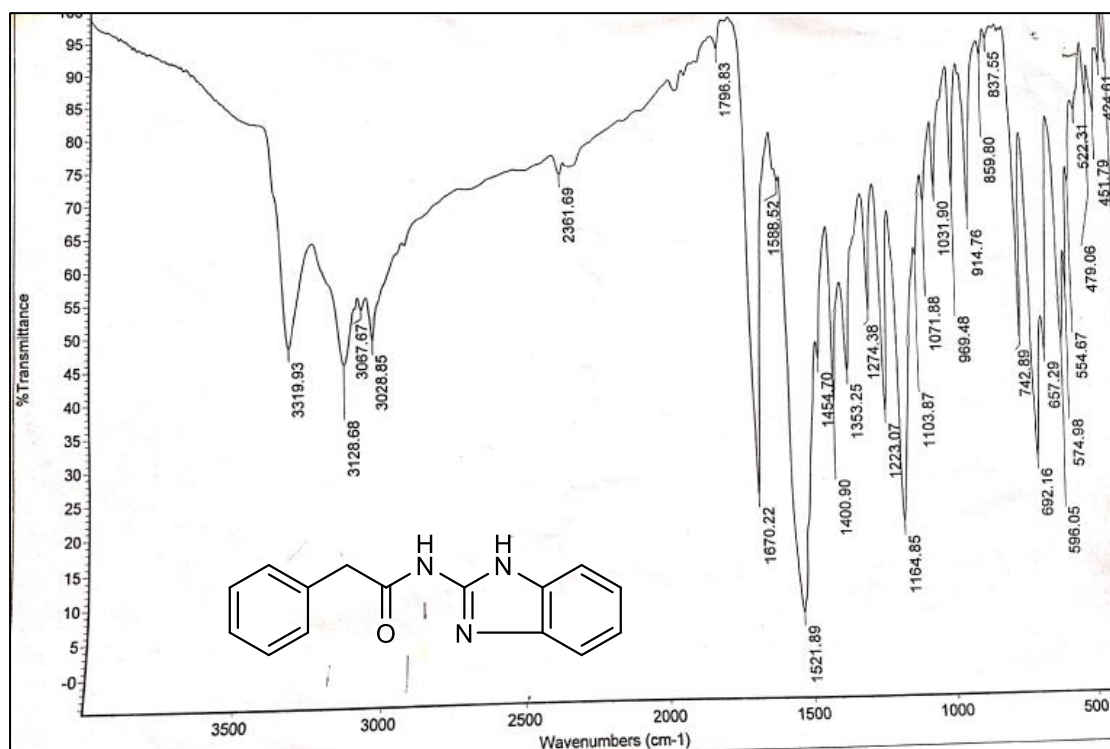
S36: Compound 2c



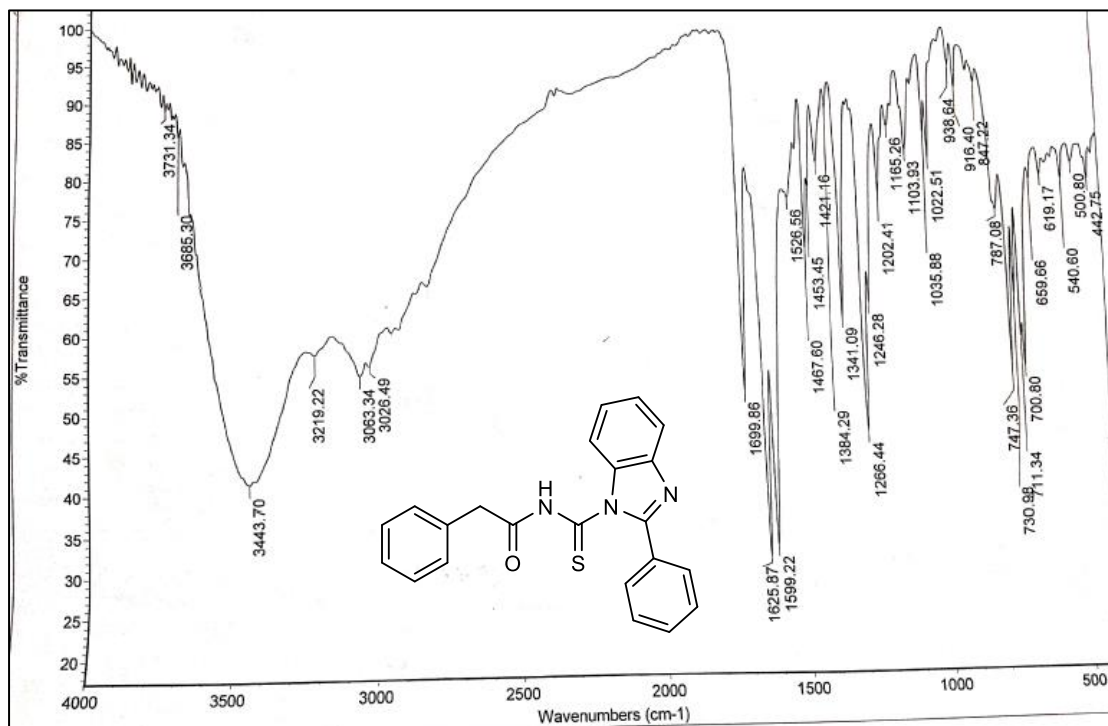
S37: Compound 2d



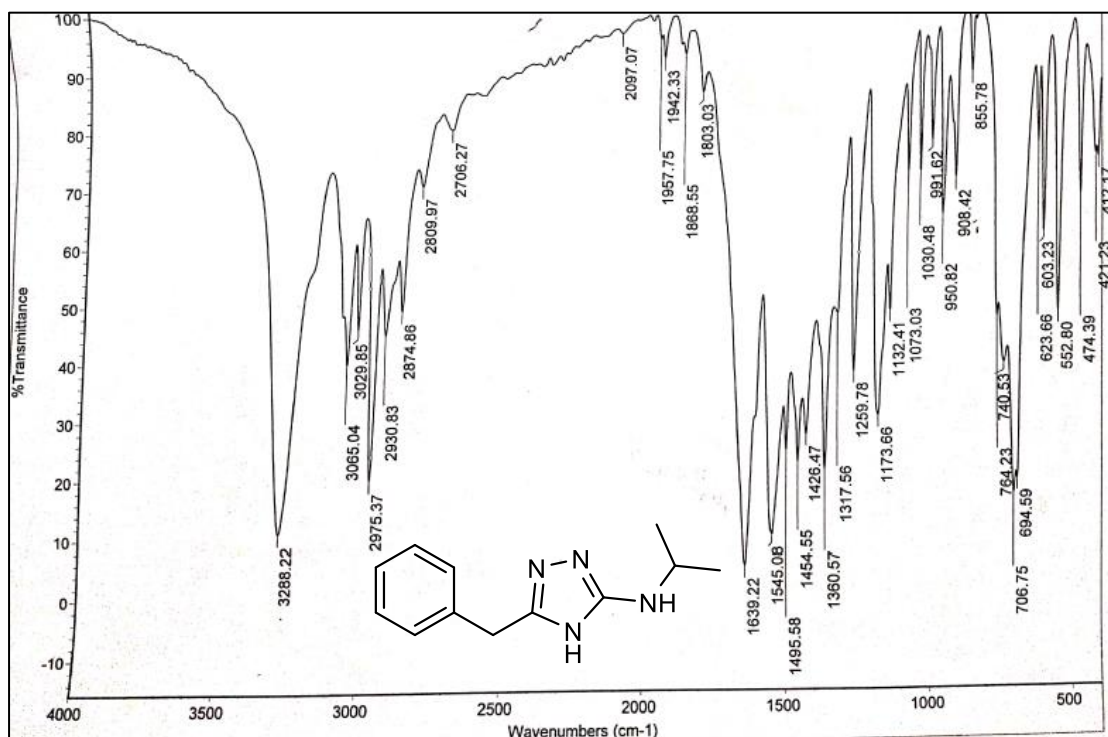
S38: Compound 2e



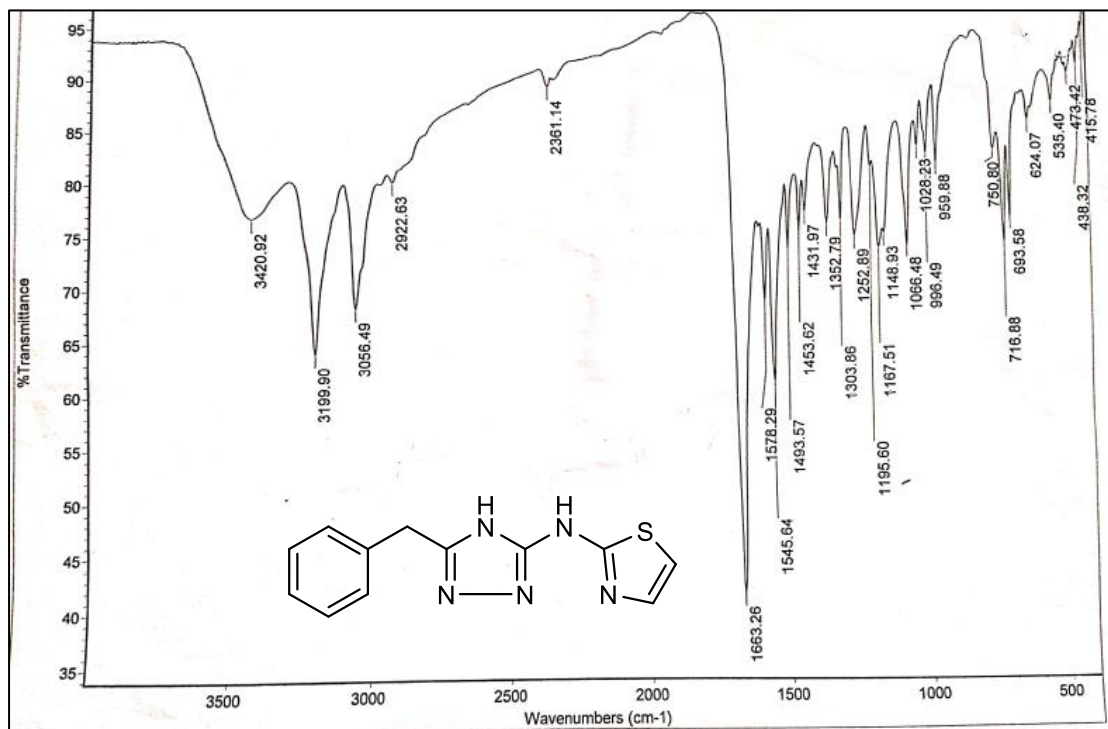
S39: Compound 3



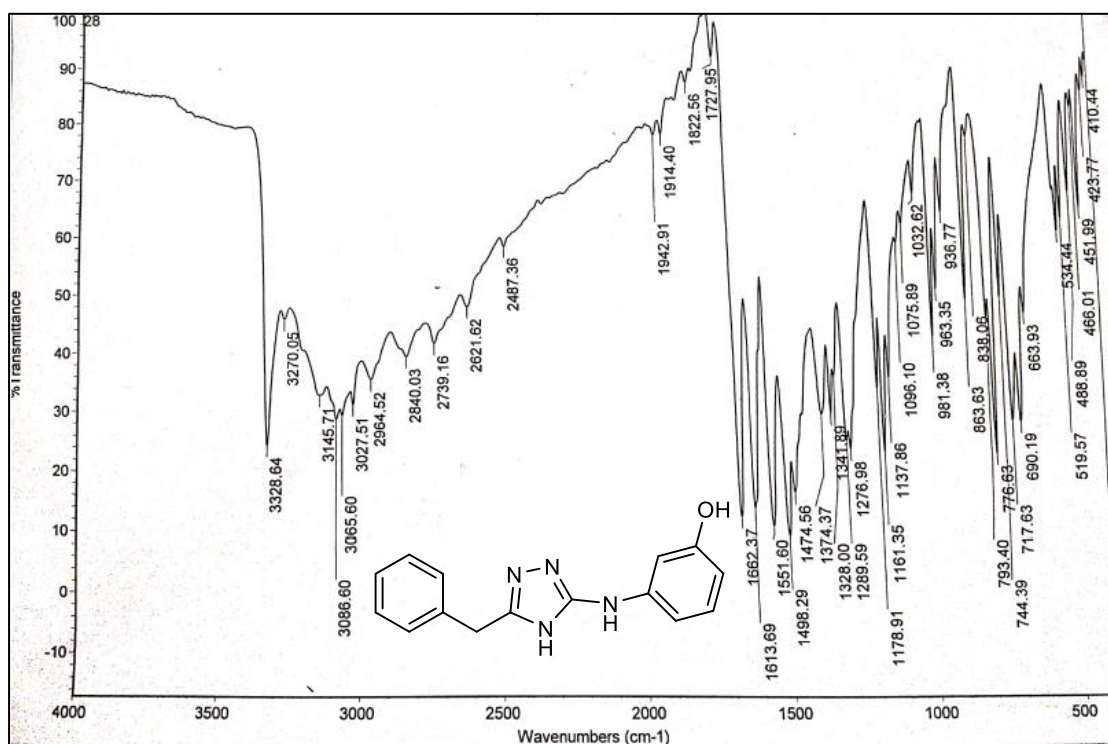
S40: Compound 4



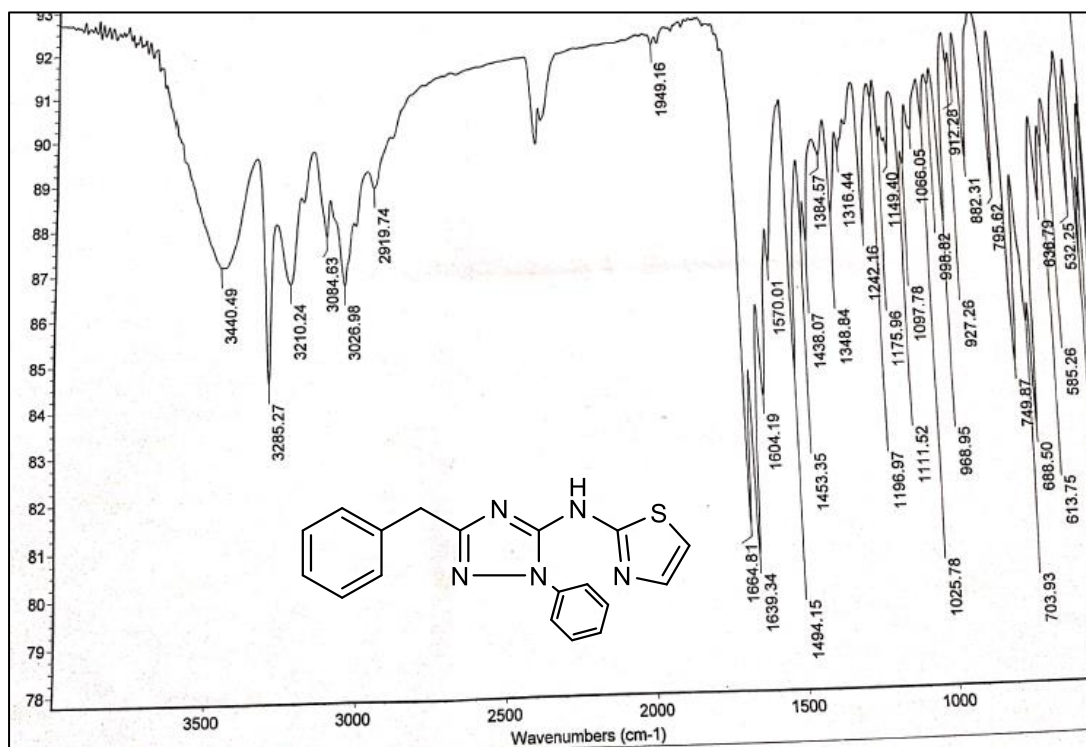
S41: Compound 5a



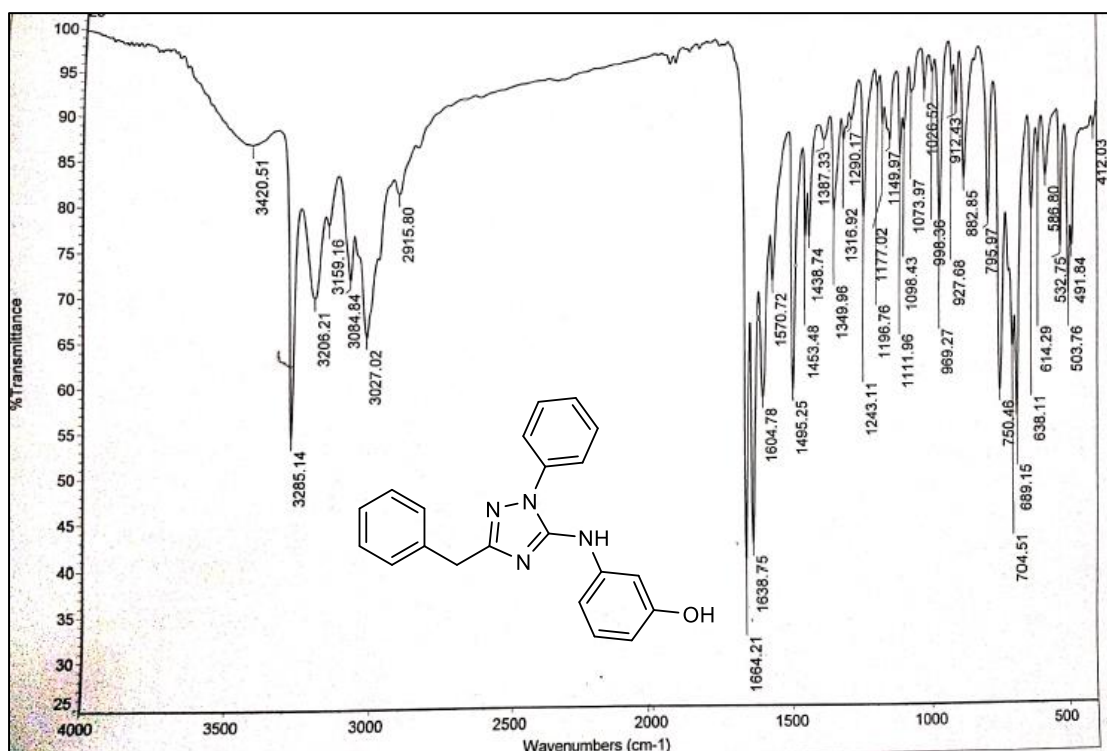
S42: Compound 5b



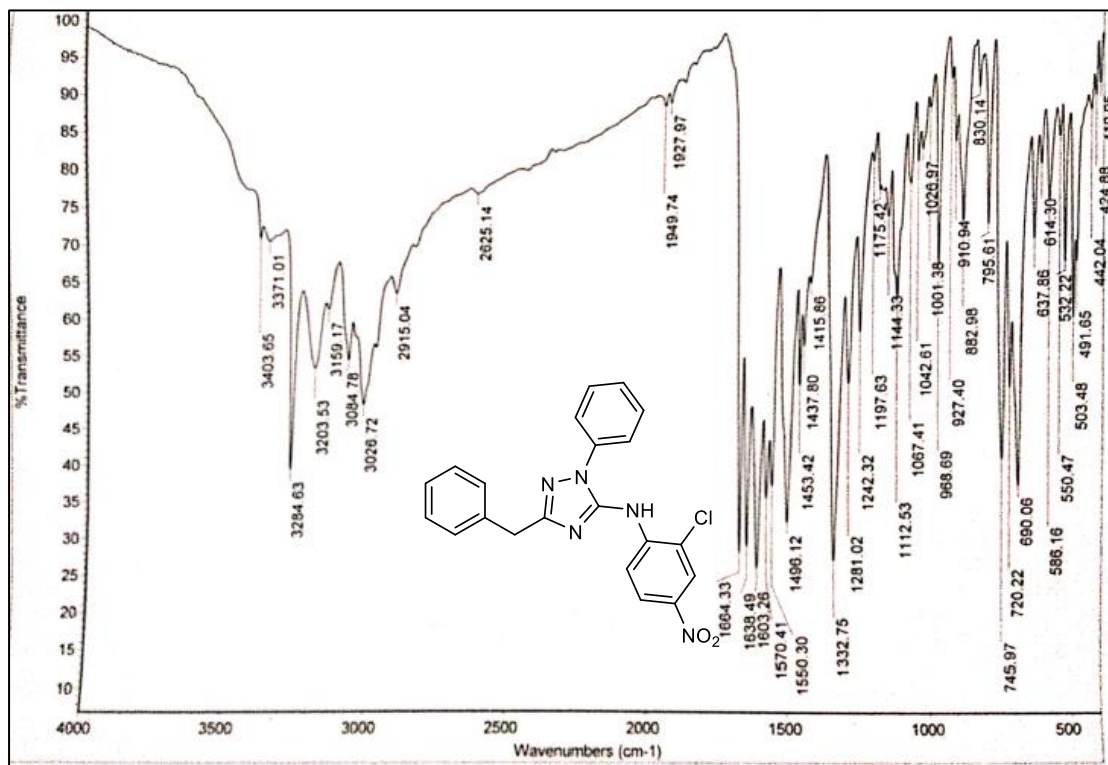
S43: Compound 5c



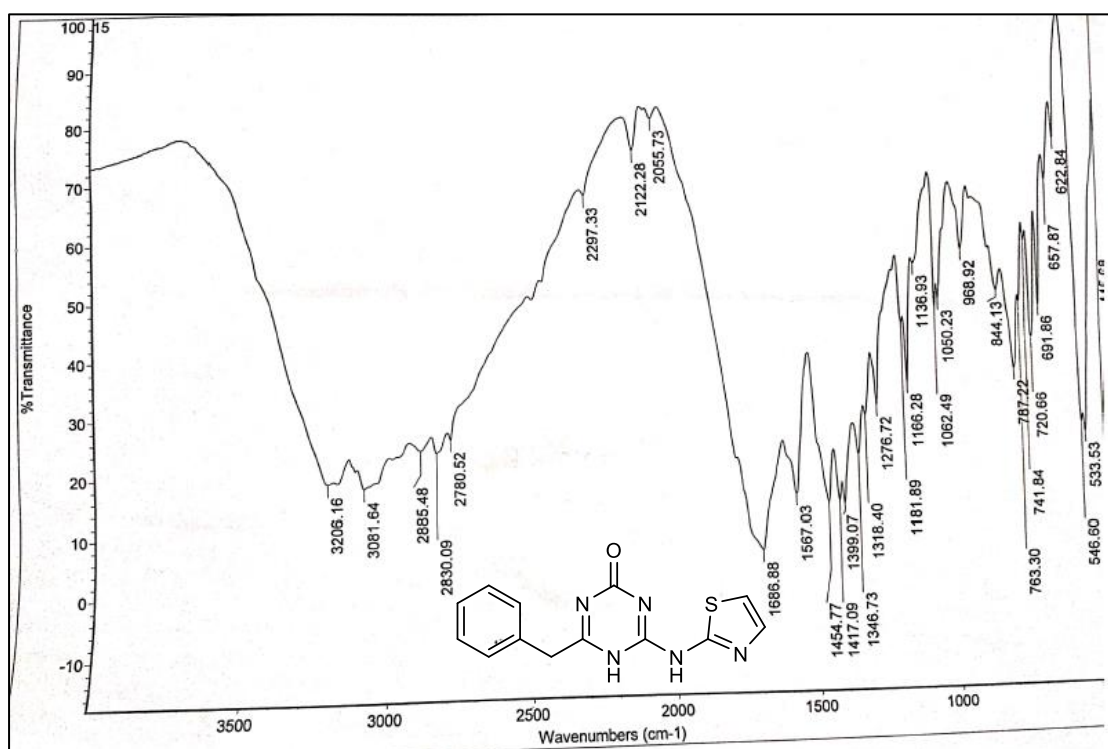
S44: Compound 6a



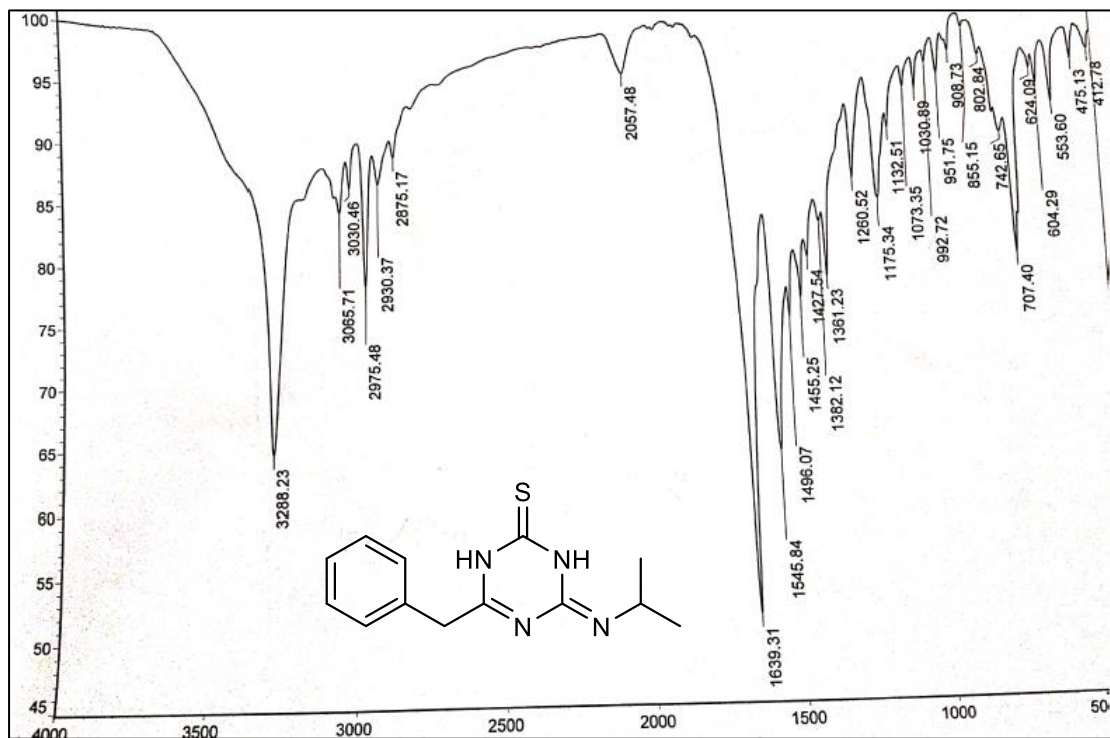
S45: Compound 6b



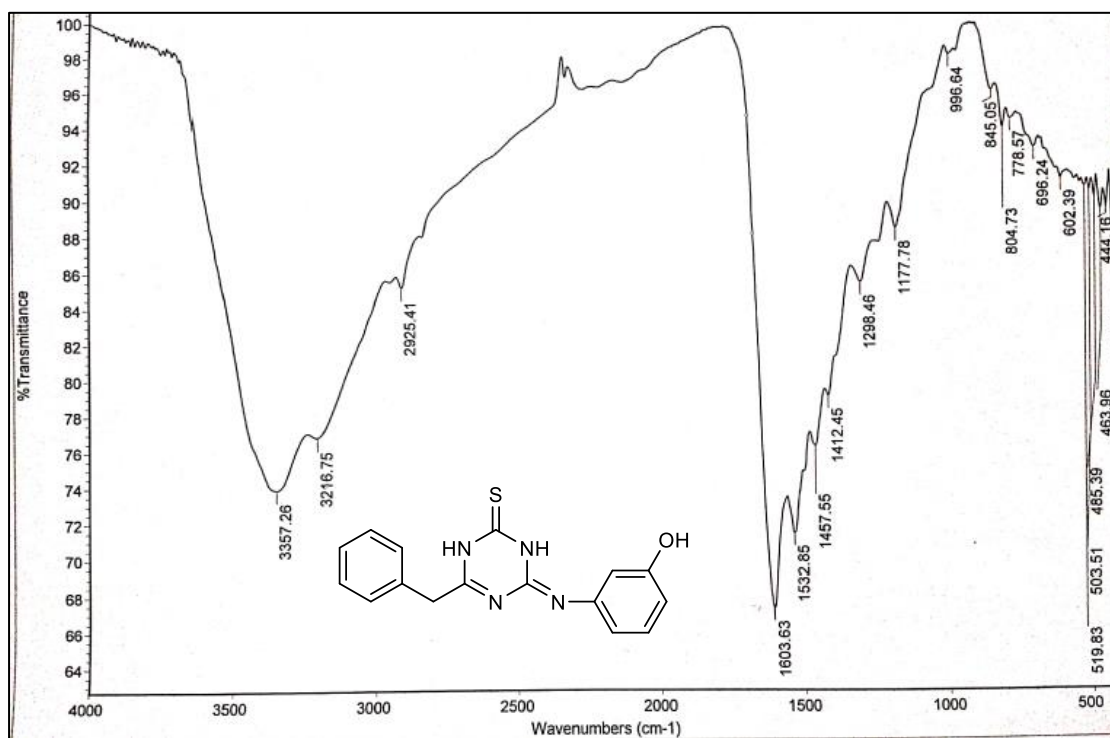
S46: Compound 6c



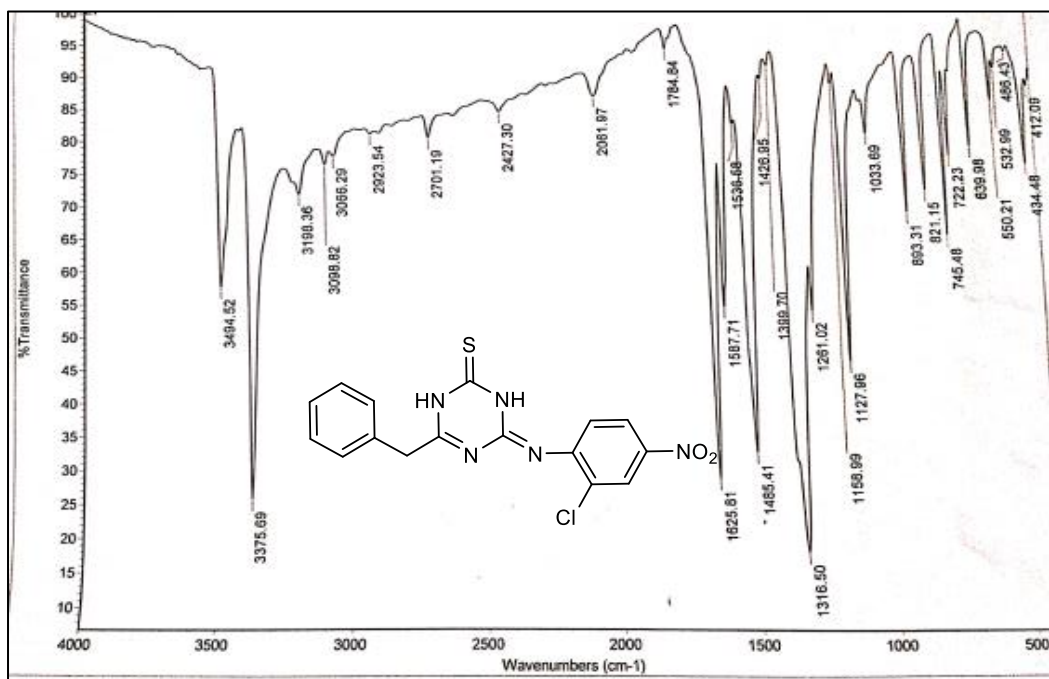
S47: Compound 7



S48: Compound 8a

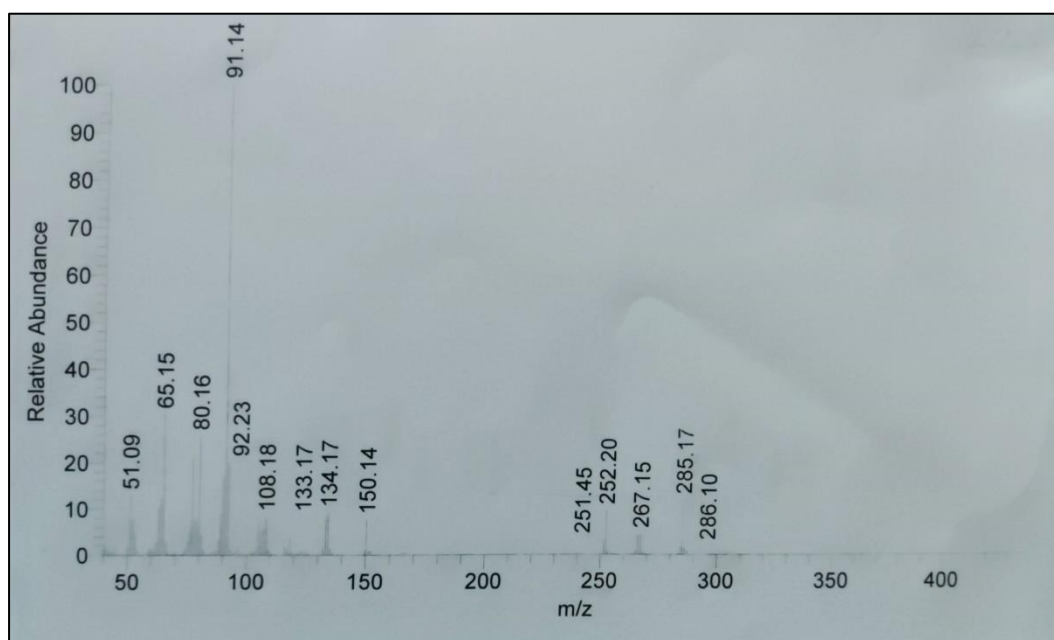


S49: Compound 8c

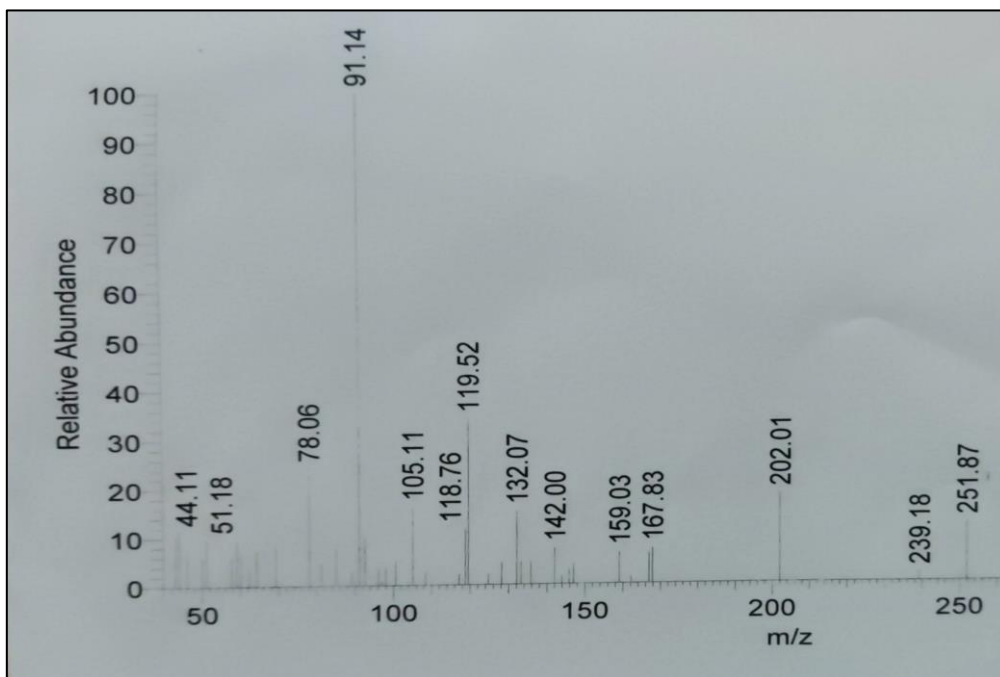


S50: Compound 8d

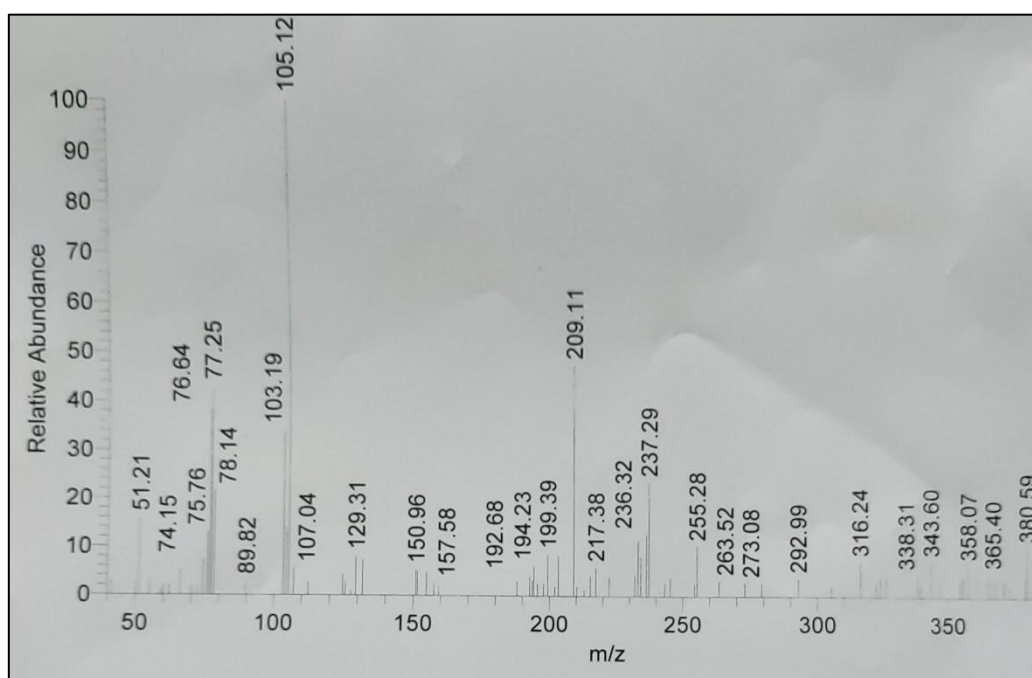
Mass spectra of the new compounds:



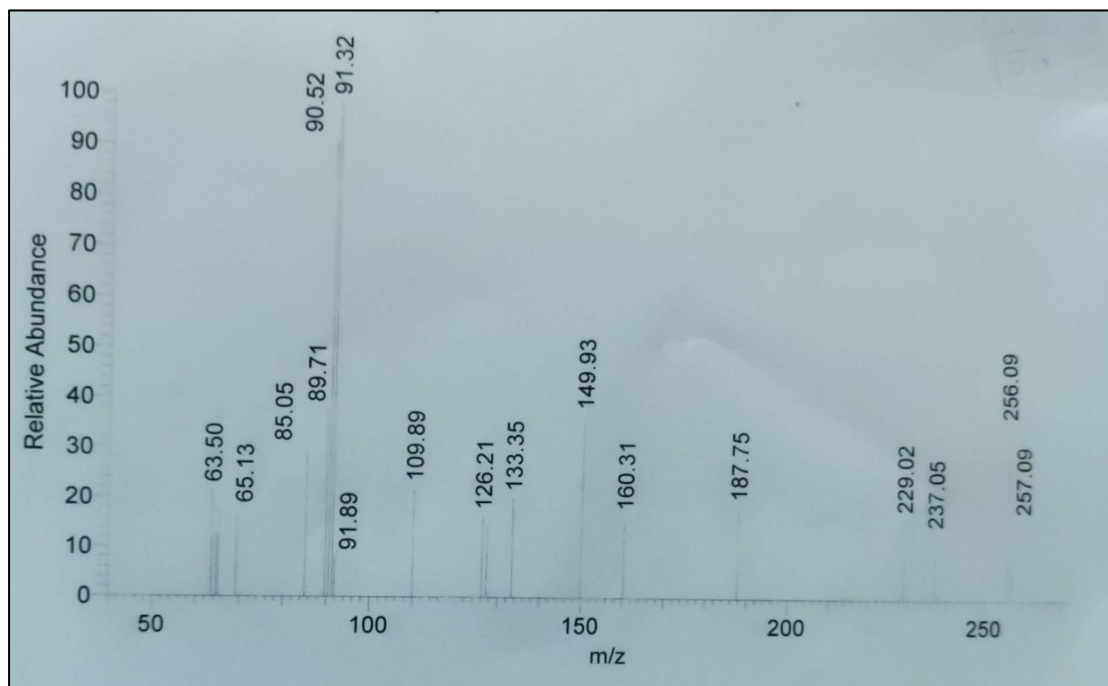
S51: Compound 2c



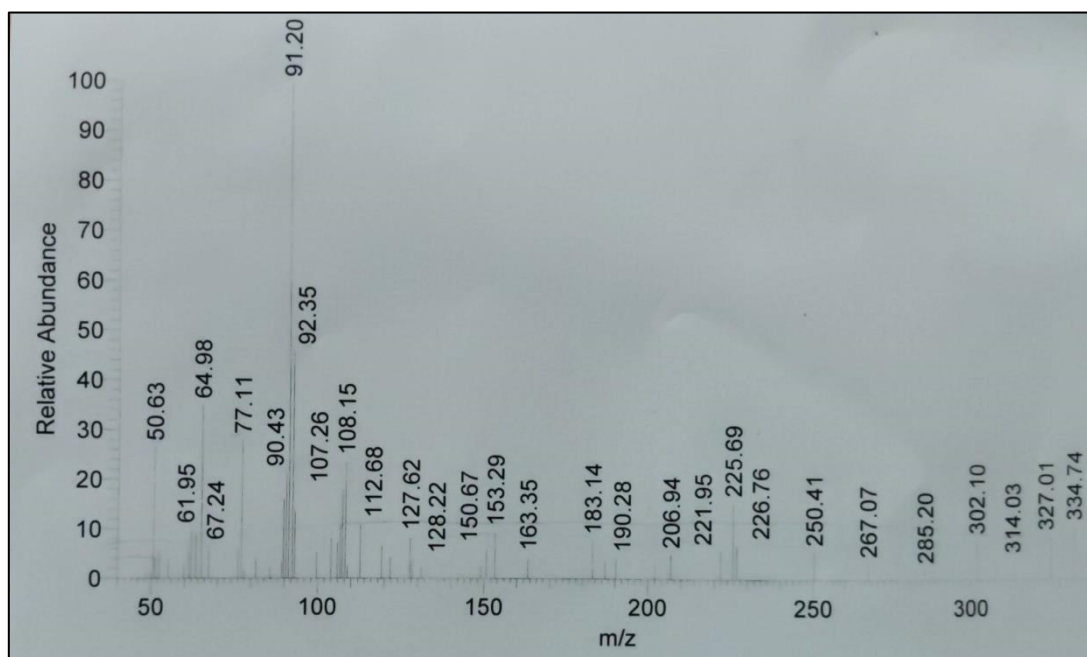
S52: Compound 3



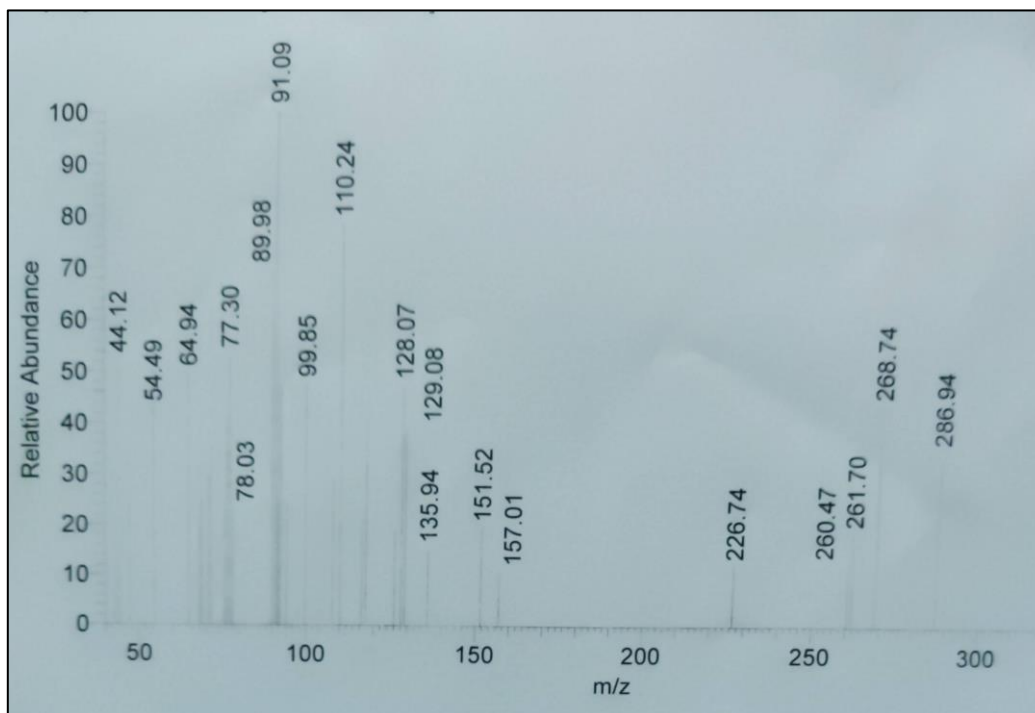
S53: Compound 4



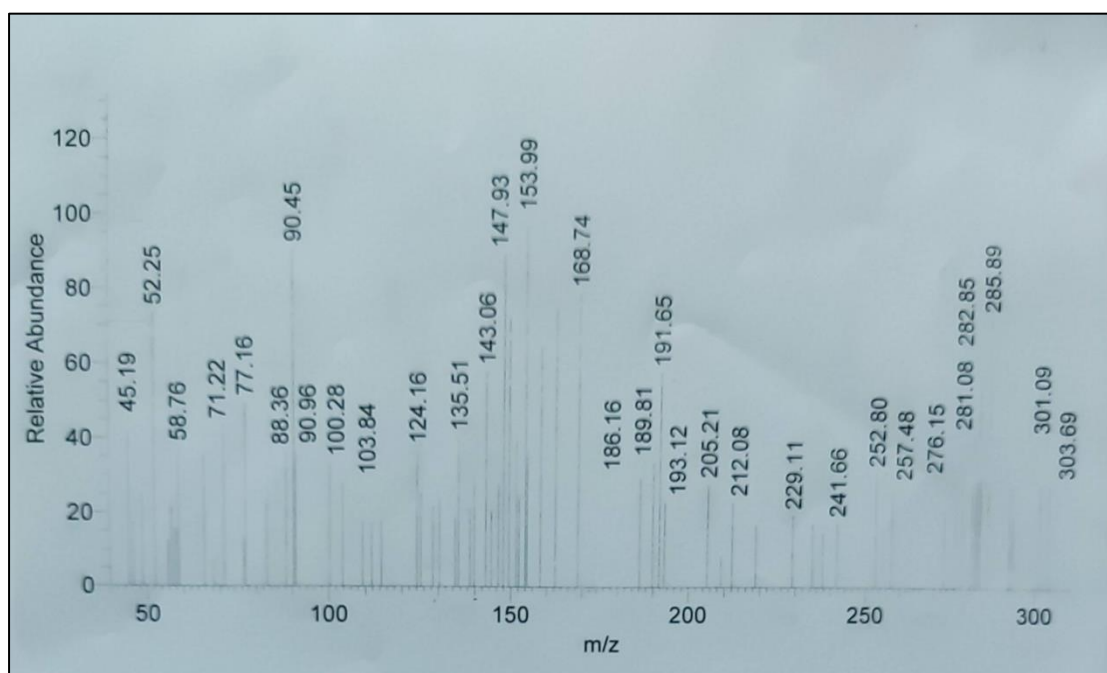
S54: Compound 5b



S55: Compound 6a



S56: Compound 7



S57: Compound 8b